Journal of Computer-Aided Molecular Design, **15:** 883–909, 2001.
KLUWER/ESCOM
© 2001 *Kluwer Academic Publishers. Printed in the Netherlands.*

High-affinity interactions of ligands at recombinant Guinea pig $5HT_7$ receptors

R. E. Wilcox[a,*], J. E. Ragan[a], R. S. Pearlman[a], M.Y-. K. Brusniak[a], R. M. Eglen[b], D. W. Bonhaus[c], T. E. Tenner, Jr.[d] & J. D. Miller[d]

[a]*College of Pharmacy, University of Texas at Austin, TX 78712, Austin, USA;* [b]*DiscoveRx Corporation, Fremont, CA 94538, USA;* [c]*Roche Biosciences, Palo Alto, CA 94304, USA;* [d]*Department of Pharmacology, Texas Tech University Health Sciences Center, Lubbock TX 79430, USA;* [e]*Department of Cell and Neurobiology, Keck School of Medicine of the University of Southern California, Los Angeles, CA 90089, USA*

Received 31 January 2001; accepted 24 May 2001

Key words: agonist affinity, computer-aided design, comparative molecular field analysis, serotonin receptors, recombinant receptors

Summary

The serotonin $5HT_7$ receptor has been implicated in numerous physiological and pathological processes from circadian rhythms [1] to depression and schizophrenia. Clonal cell lines heterologously expressing recombinant receptors offer good models for understanding drug-receptor interactions and development of quantitative structure-activity relationships (QSAR). Comparative Molecular Field Analysis (CoMFA) is an important modern QSAR procedure that relates the steric and electrostatic fields of a set of aligned compounds to affinity. Here, we utilized CoMFA to predict affinity for a number of high-affinity ligands at the recombinant guinea pig $5HT_7$ receptor. Using R-lisuride as the template, a final CoMFA model was derived using procedures similar to those of our recent papers [2, 3, 4] The final cross-validated model accounted for >85% of the variance in the compound affinity data, while the final non-cross validated model accounted for >99% of the variance. Model evaluation was done using cross-validation methods with groups of 5 ligands. Twenty cross-validation runs yielded an average predictive $r^2(q^2)$ of 0.779 ± 0.015 (range: 0.669–0.867). Furthermore, 3D-chemical database search queries derived from the model yielded hit lists of promising agents with high structural similarity to the template. Together, these results suggest a possible basis for high-affinity drug action at $5HT_7$ receptors.

Abbreviations: 5-Carboxamidotryptamine (5-CT); 5-HT (5-hydroxytryptamine, serotonin); 5-methoxytryptamine (5-MET); 8-OH-DPAT, R- and S-8-hydroxy-dipropyl-amino-tetraline hydro-bromide; ACD, Available Chemical Directory; APO, R-apomorphine; bulbocapnine, (+)-bulbocapnine; CoMFA, comparative molecular field analysis; CoMSIA, Comparative Molecular Similarity Indices Analysis; K_L, low-affinity agonist dissociation constant, CMC, Comprehensive Medicinal Chemistry; lisuride, R-lisuride; mCPP, 1-(3-chloro-phenyl)piperazine; Maybridge; MDDR, Modern Drug Data Report; NCI, national cancer institute; NPA, R-N-n-propylnorapomorphine; QSAR, quantitative structure-activity relationship; SEE, standard error of the estimate; SEP, standard error of prediction.

Introduction

The serotonin-7 ($5HT_7$) receptor represents the most recent [1, 5] and certainly one of the more intriguing members of the serotonin receptor family [6, 7]. There are several reasons for such an interest in the $5HT_7$ receptor. First, it is expressed in many species, resulting in cloning from rat brain [1, 8, 9], guinea pig [10], and *Drosophila* [11]. Second, the $5HT_7$ receptor appears implicated in a number of diseases and physiologi-

*To whom correspondence should be addressed. E-mail: wilcoxrich@mail.utexas.edu

Table 1. Affinities of training set compounds at recombinant $5HT_7$ receptors

Drug	Measured K_d (M)	Predicted K_d (M)
Training set		
5-Methoxytryptamine	5.01E−10	4.96E−10
5CT	5.25E−10	5.21E−10
5HT	8.71E−10	8.84E−10
Amesergide	7.80E−08	7.87E−08
Apomorphine	5.62E−07	5.52E−07
Bromocriptine	1.07E−08	1.08E−08
Bulbocapnine	2.69E−07	2.71E−07
Ergotamine	5.01E−08	5.00E−08
Laurolistine	3.31E−07	3.34E−07
R-Lisuride	9.50E−09	9.58E−09
LY215840	1.47E−08	1.48E−08
LY53857	1.02E−07	9.89E−08
NPA	6.92E−07	6.99E−07
Oxymetazoline	5.01E−08	4.97E−08
Sergolexole	1.01E−07	1.02E−07
R-8OHDPAT	3.50E−08	1.35E−08
Terguride	1.00E−08	1.63E−08

Table 2. Literature values for affinity of 8-OH-DPAT

Isomer	K_i (nM)	Reference
RS	35 K_i	9
RS	52 K_i	8
R	81–141 K_i	7
R	5623 EC50 cyclase	7
R	5200 EC50 cyclase	10
RS	2300 EC50 cyclase	1
RS	62% Intrinsic activity	1
RS	466 K_i	11
R	39–501 K_i	6

cal processes including migraine [12], psychosis [13], depression [14], gastrointestinal functions [15], and circadian rhythms [1]. The pharmacology of the $5HT_7$ receptor is especially interesting to investigators interested in drug development because of its high affinity for a number of antidepressants [14], antipsychotics (both typical and atypical) and antiparkinson agents [1, 8–11].

The ability to activate $5HT_7$ receptors selectively represents a goal with both theoretical and clinical significance. Development of compounds to achieve this goal and an understanding of the regulation of the $5HT_7$ receptor can proceed more effectively if the molecular bases for agonist and antagonist interactions with the $5HT_7$ receptor are understood. The method of Comparative Molecular Field Analysis (CoMFA) is one technique that has been shown to be effective in increasing the understanding of drug-receptor interactions at a variety of receptors. In this procedure compounds are aligned according to a specific rule (the alignment rule). One approach to this process is to align compounds with a template molecule using flexible-field fit methods. Then the CoMFA procedure computes the steric and electrostatic intermolecular interaction fields of 3D-grid points surrounding the aligned ligands. Finally, the partial least squares (PLS) regression method is used to derive an optimum CoMFA model relating the computed interaction potentials to measured, and, subsequently, predicted activities. Typically such CoMFA models have high predictive validity [2–4]. These models also have useful qualitative features in that the contour map of the steric and electrostatic fields associated with the model provides insights regarding the receptor site of interest.

In the present report we sought to develop a CoMFA model for potential agonist compounds interacting at the $5HT_7$ receptor. High-affinity compounds having interesting 2D- and 3D- structural features were selected and those compounds thought to possess at least some agonist activity were retained for a final CoMFA. The CoMFA model derived from these compounds appears to have good cross-validation characteristics. Furthermore, the model has yielded sufficient information to allow formulation of productive search queries of several 3D-chemical databases. Finally, the model shows interesting similarities and contrasts with previously derived models for agonist affinity at D_1 and D_2 dopamine [2–4] and $5HT_{1A}$ receptors.

Methods

Cell culture

Chinese hamster ovary (CHO) cells transfected with the guinea pig $5HT_7$ receptor were grown to near-confluence in a modified F-12 medium, containing 10% w/v fetal calf serum, 1% w/v penicillin/streptomycin and 0.3 mg/ml geneticin (5% CO_2, 37 °C) in polystyrene flasks. CHO cells (3–17 $\times$ 10^6) were disrupted in lysis buffer (Tris, MgSO4, and Na_2EDTA), membranes were isolated by centrifugation at 39 000 *g* for 10 min at 4 °C, and resuspended in

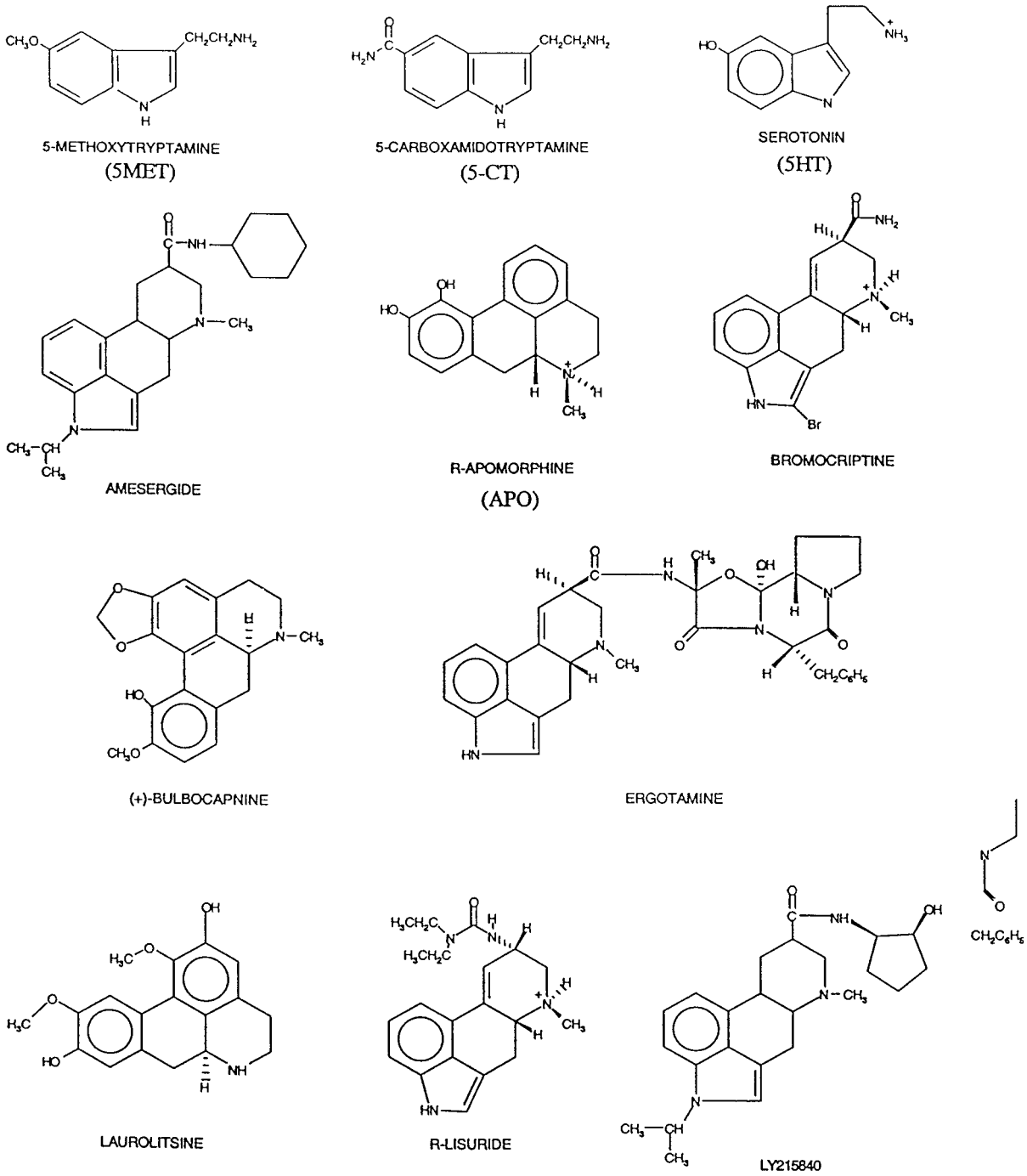

Figure 1. 2D Structures of the training set compounds.

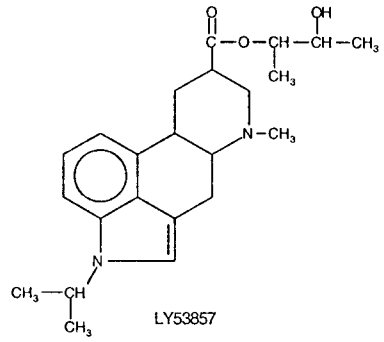

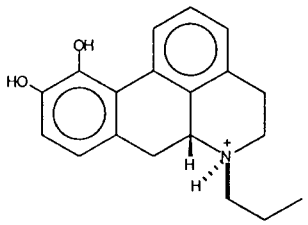

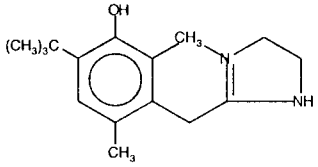

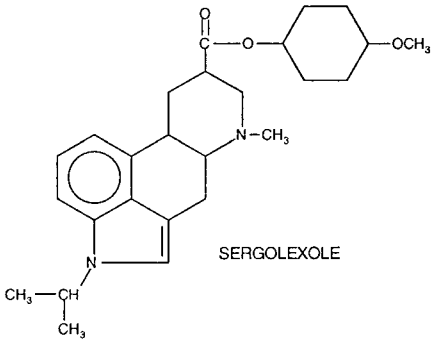

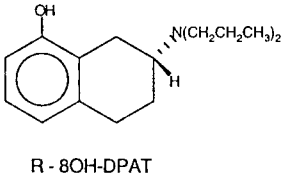

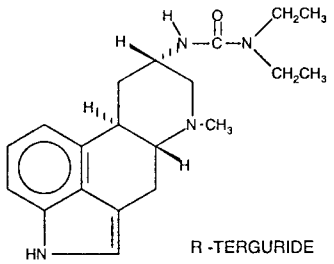

Figure 1. Continued.

STEEDS buffer according to Tsou [10]. Membranes were frozen in 1 ml aliquots of approximately 1 mg/ml protein concentration.

Compounds used

5-Carboxamidotryptamine (5-CT), 5-methoxytryptamine (5-MeOT), methylsergide maleate, 5-hydroxytryptamine (5-HT) hydrochloride, and 8-hydroxydipropylaminotetraline hydrobromide (8-OH-DPAT) were purchased from Research Biochemicals International (Natick, MA). (^{3}H)-5-CT (50.4 Ci/mmol) was purchased from Dupont/New England Nuclear (Boston, MA). All chemicals used for adenylate cyclase assays were purchased from Sigma. Radiolabeled ATP for the adenylate cyclase assays was purchased from New England Nuclear.

Compound affinities at recombinant 5HT$_7$ receptors

Affinities of potential ligands were measured at recombinant 5HT$_7$ receptors as described below [7]. The gene product was originally cloned from cDNA of guinea pig hippocampus [10] and stably expressed in CHO cells. Some of the compound affinity values have been reported previously [7]. Additionally, affinities of four additional 5HT$_7$ receptor ligands were obtained from the literature (amesurgide, LY53857, LY215840,

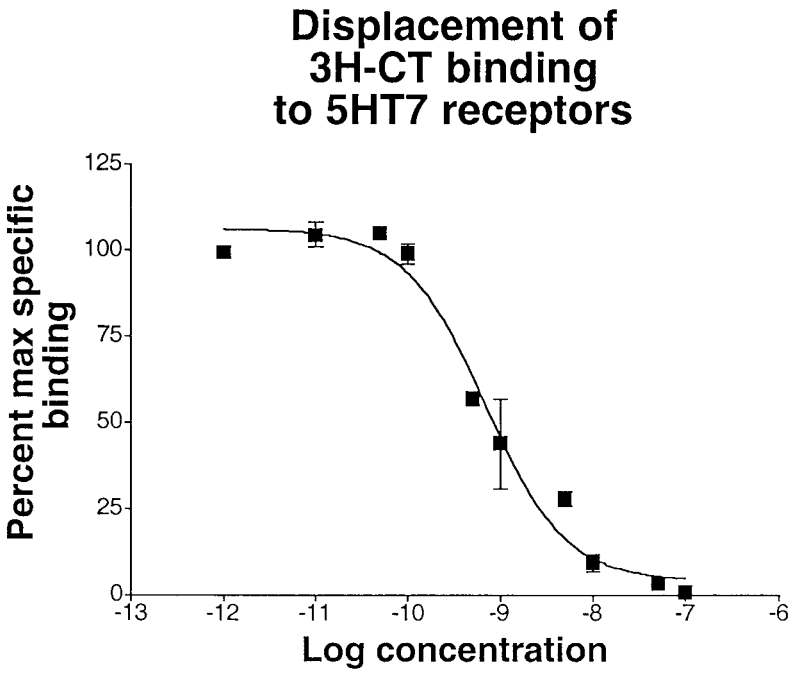

Figure 2. Displacement of 3H-5CT by 5HT at recombinant 5HT7 receptors in CHO cells. Shown are the results of a single experiment in duplicate.

and sergolexole) [16]. A training set of 17 compounds was utilized for the present study. Affinities of these compounds are provided in Table 1.

For saturation studies using radioligand binding methods, membranes were incubated for two hours at room temperature with 0.05–10 nM (^{3}H)-5-CT (51.3 Ci/mmol New England Nuclear, Boston) in STEEDS buffer. To each assay tube were added 200 µl cell membrane, 100 µl radioligand, 150 µl buffer and 50 µl of buffer (total binding) or 50 µl of 1 µM 5-HT, to define non-specific binding. For competition studies, membranes were incubated with 0.3–0.7 nM (^{3}H)-5-CT for two hours with or without competing ligands. Duplicate assays were run using ten concentrations of competing ligand at approximately equal log intervals from 10^{-12} to 10^{-7} or 10^{-10} to 10^{-5} M depending on the ligand in addition to total and nonspecific binding. To each assay tube, 200 µl cell membrane, 100 µl radioligand, 150 µl buffer and an additional 50 µl of buffer (for total binding), 50 µl of 1 µM 5-HT (for nonspecific binding) or 50 µl of displacing compounds were added. Assays were terminated by rapid filtration through 0.3% polyethylenimine pretreated GF/B filters, washed twice with 1 ml ice cold 50 mM Tris-base, pH 7.4. Bound radioactivity was determined by liquid scintillation spectrophotometry using a Packard Topcount scintillation counter. IC_{50} values were obtained by non-linear regression. The inhibition dissociation constant (K_i) of each compound was then determined according to the method of Cheng and Prusoff [46].

Adenylyl cyclase assay

Adenylyl cyclase activity was determined according to the method of Salomon. [17] There were only minor alterations in the protocol. Briefly, CHO cell membranes (20 µg) were incubated for 20 min at 30 °C in a final volume of 50 µl of buffer. The buffer contained Tris acetate (25 mM, pH 7.6), magnesium acetate (5 mM), ATP (0.1 mM), cyclic AMP (0.05 mM), dithiothreitol (1 mM), BSA (0.1 mg/ml), GTP (0.01 mM), creatine phosphate (5 mM), creatine phosphokinase (50 U/ml), and ($\alpha-^{32}$P) ATP (1 µCi). The reaction was stopped by the addition of 100 µl of stopping solution containing 2% sodium lauryl sulfate, ATP (45 mM), and 3′5′-cyclic AMP (1.3 mM). (^{3}H) Cyclic AMP (~10 000 cpm) was added to monitor the recovery of (^{32}P) cyclic AMP. Formed (^{32}P) cyclic AMP and (^{3}H) cAMP were isolated by dual-column (dowex, alumina) chromatography. Samples were boiled for 5 min, each poured over a Dowex column that was washed with 0.5 ml H_2O, and the

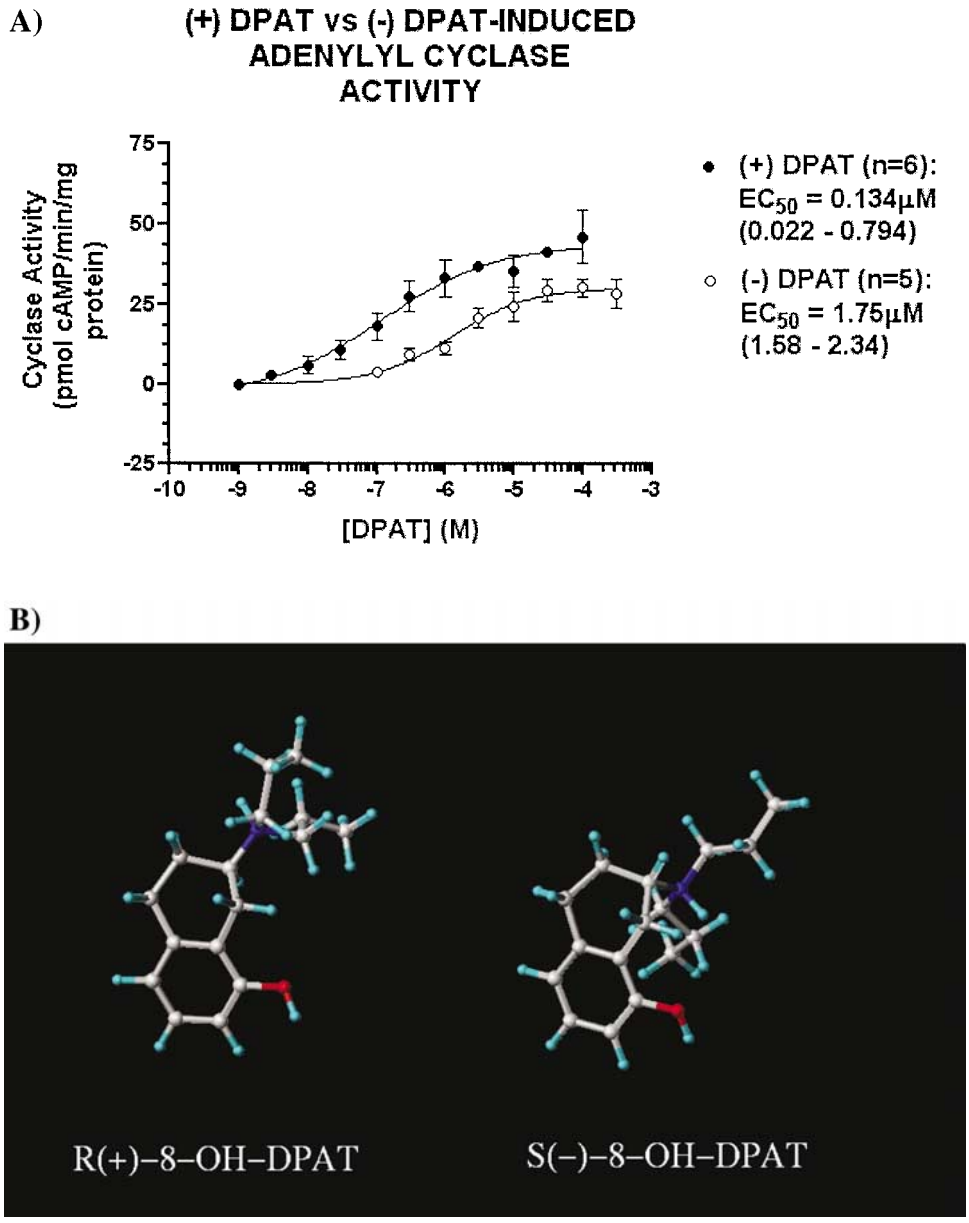

Figure 3. Adenylate cyclase activity of 8-OH-DPAT. (A) Comparison of adenylate cyclase activity of R- and S-8-OH-DPAT. (B) Structural comparison of R- and S-8-OH-DPAT.

effluent was discarded. The Dowex column was then washed with 4 ml H_2O into an alumina column, which was subsequently washed with 1.25 ml of 0.1 M imidazole buffer (pH 7.3), discarding the effluent. The column was washed a final time with 2.5 ml imidazole buffer, with the effluent collected into a scintillation vial with fluor added for counting. The cAMP production was calculated as pmol/mg protein/min. Results were expressed as the change in activity, which was calculated as ligand-stimulated minus basal activity. Responses were quantified by dual channel liquid scintillation counting using a Packard model 1900 TR liquid scintillation analyzer. Results were converted to the mean ± SEM. EC_{50} values were calculated according to Fleming [18] and reported as the geometric mean ±95% confidence intervals. The Student's *t*-test was used to determine statistical differences be-

Table 3. Distance information for training set ligands at recombinant $5HT_7$ receptors

Drug	N+ − H-bond 1 (N)	N+ − H-bond 2	N+ − centroid	N+ − plane (height)	Energy w/ electrostatics	Energy (local minimum)
5CT	5.796	–	4.992	4.35 e−01	26.98	23.91
5HT	5.905	–	4.884	9.54 e−01	26.64	23.83
5MET	5.995	–	4.953	9.96 e−01	31.97	27.30
Amesurgide	5.905	–	4.842	1.08 e+00	45.57	38.49
Apomorphine	6.547 mOH	7.891 pOH	5.192	6.61 e−01	28.03	21.35
Bromocriptine	5.980	–	4.888	3.74 e−01	39.54	35.00
Bulbocapnine	6.482 mOH	7.833 pOH	5.173	1.23 e+00	39.10	35.04
Ergotamine	5.978	–	4.891	4.48 e−01	60.91	55.32
Laurolistine	7.415 mOH	7.766 pOH	5.167	1.39 e−01	34.60	16.00
Lisuride R+	5.965	–	4.883	5.13 e -01	33.15	33.15
LY215840	5.965	–	4.883	5.13 e−01	57.61	47.92
LY53857	5.963	–	4.886	9.03 e−01	48.10	41.65
NPA	6.603 mOH	7.933 pOH	5.223	4.72 e−01	37.63	26.44
Oxymetazoline	7.197	–	4.929	4.64 e−01	21.10	19.87
Sergolexole	5.979	–	4.891	6.33 e−01	49.16	42.08
R-8OHDPAT	4.901	–	5.055	1.38e+00	38.88	29.95
R-Terguride	5.965	–	4.886	7.26e−01	33.68	30.27

Distances and plane heights are in Å. Energy is in kcal/mol.

Table 4. CoMFA results for ligand affinity at recombinant $5HT_7$ receptors

Fields (E cutoff kcal per mole)	Dielectric function	Min. σ	Grid step size (Å)	Probe atom type	# col	q2 (SEP)	# PC	CoMFA grid box
Steric 30/Elec 30	1/r	2.0	2.0	Csp3+	358	0.583 (1.863)	6	Auto[a]
Steric 30	1/r	2.0	2.0	Csp3+	226	0.541(1.995)	4	Auto
Elec. 30	1/r	2.0	2.0	Csp3+	202	0.734 (1.488)	6	Auto
Both 20/20	1/r	2.0	2.0	Csp3+	330	0.656 (1.691)	6	Auto
Both 10/10	1/r	2.0	2.0	Csp3+	247	0.734 (1.487)	6	Auto
Both 25/25	1/r	2.0	2.0	Csp3+	351	0.588 (1.852)	6	Auto
Both 15/15	1/r	2.0	2.0	Csp3+	183	0.743 (1.463)	6	Auto
Steric 20/Elec 15	1/r	2.0	2.0	Csp3+	307	0.698 (1.584)	6	Auto
Steric 15/Elec 10	1/r	2.0	2.0	Csp3+	253	0.745 (1.389)	5	Auto
Steric 15/Elec 10	**1/r**	**1.75**	**2.0**	**Csp3+**	**274**	**0.851 (1.061)**	**5**	New region[b]
Steric 15/Elec 10	1/r	1.75	2.2	Csp3+	221	0.753 (1.434)	6	New region
Steric 15/Elec 10	1/r	1.75	1.8	Csp3+	400	0.833 (1.180)	6	New region
Steric 15	1/r	1.75	2.0	Csp3+	223	0.782 (1.346)	6	New region
Elec 10	1/r	1.75	2.0	Csp3+	165	0.756 (1.424)	6	New region
Steric 15/Elec 10	1/r	1.75	2.0	O_{2-}	277	0.842 (1.146)	6	New region
Steric 15/Elec 10	1/r	1.75	2.0	H+	282	0.842 (1.145)	6	New region
Steric 15/Elec 10	C	1.75	2.0	Csp3+	223	0.782 (1.346)	6	New region
Region Focus[c]	1/r	1.75	2.0	Csp3+	112	0.808 (1.265)	6	New region
Steri 15/Elec 10 CoMSIA[d]	1/r	1.75	2.0	Csp3+	1021	0.856 (1.096)	6	New region

[a]The auto CoMFA grid box had coordinates X (−13.19, 8.84), Y (−10.28, 16.30), and Z (−12.79, 5.45).
[b] Optimal grid box position was as follows: X (−13.79, 8.54), Y (10.73, 16.15), and Z (−12.44, 5.45)
[c]Default discriminant function setting (power = 0.3).
[d]CoMSIA included electrostatic, hydrophobic, steric, donor and acceptor components.
PC = principal components.

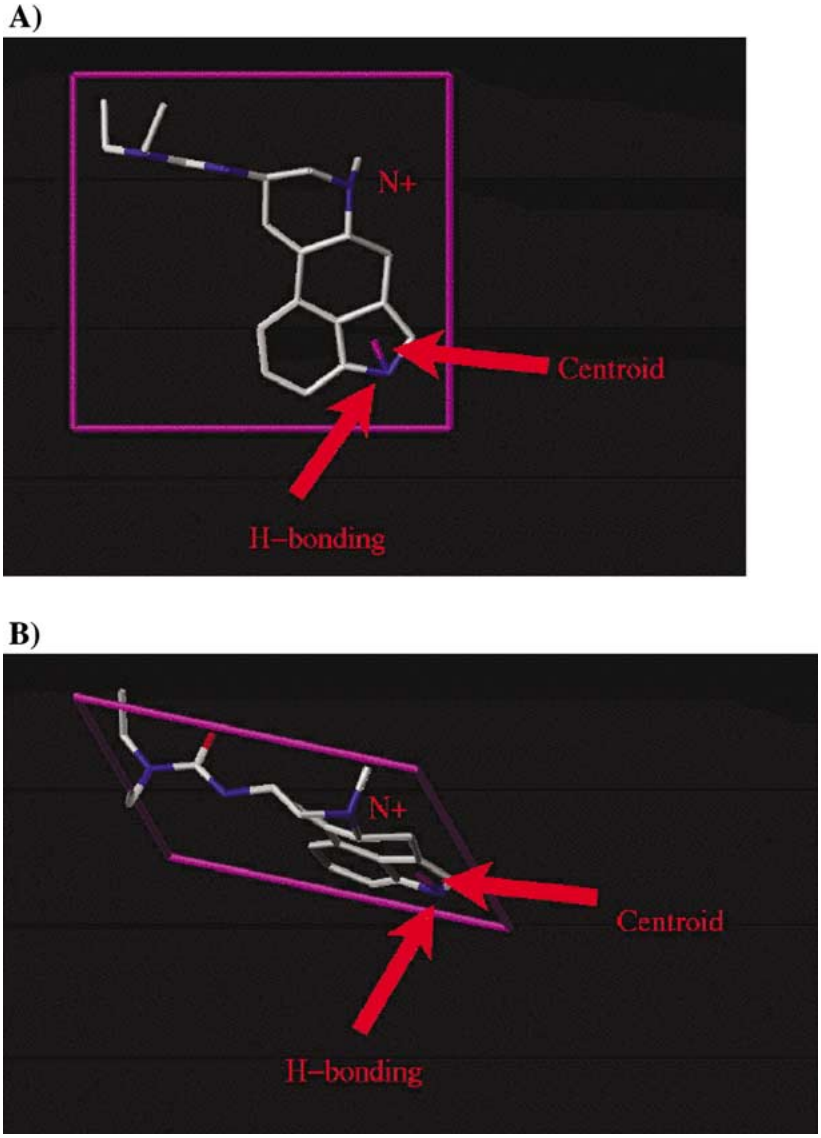

Figure 4. Distance information. (A) Top view. (B) Side view.

tween log EC_{50} values for the DPAT (+) and (−) enantiomers.

Computational chemistry

Overview of the approach

For all CoMFA, Region Focusing, and CoMSIA (Comparative Molecular Similarity Indices Analysis) studies, initial conformations for training set ligand alignment were established using CONCORD [19, 20]. Conformations of each compound were minimized using the MAXIMIN2 procedure within SYBYL [21]. Flexible-field fit methods were then utilized to determine the conformations of the training set compounds that matched the template [2–4]. CoMFA was performed using the procedures provided within SYBYL [2–4].

For the CoMFA we utilized R-lisuride, a high-affinity and conformationally constrained $5HT_7$ receptor agonist, as the template (Figure 1). 5-CT also has very high affinity for the $5HT_7$ receptor. However, its structure (Figure 1) is highly flexible, with a large number of possible candidate binding conformations

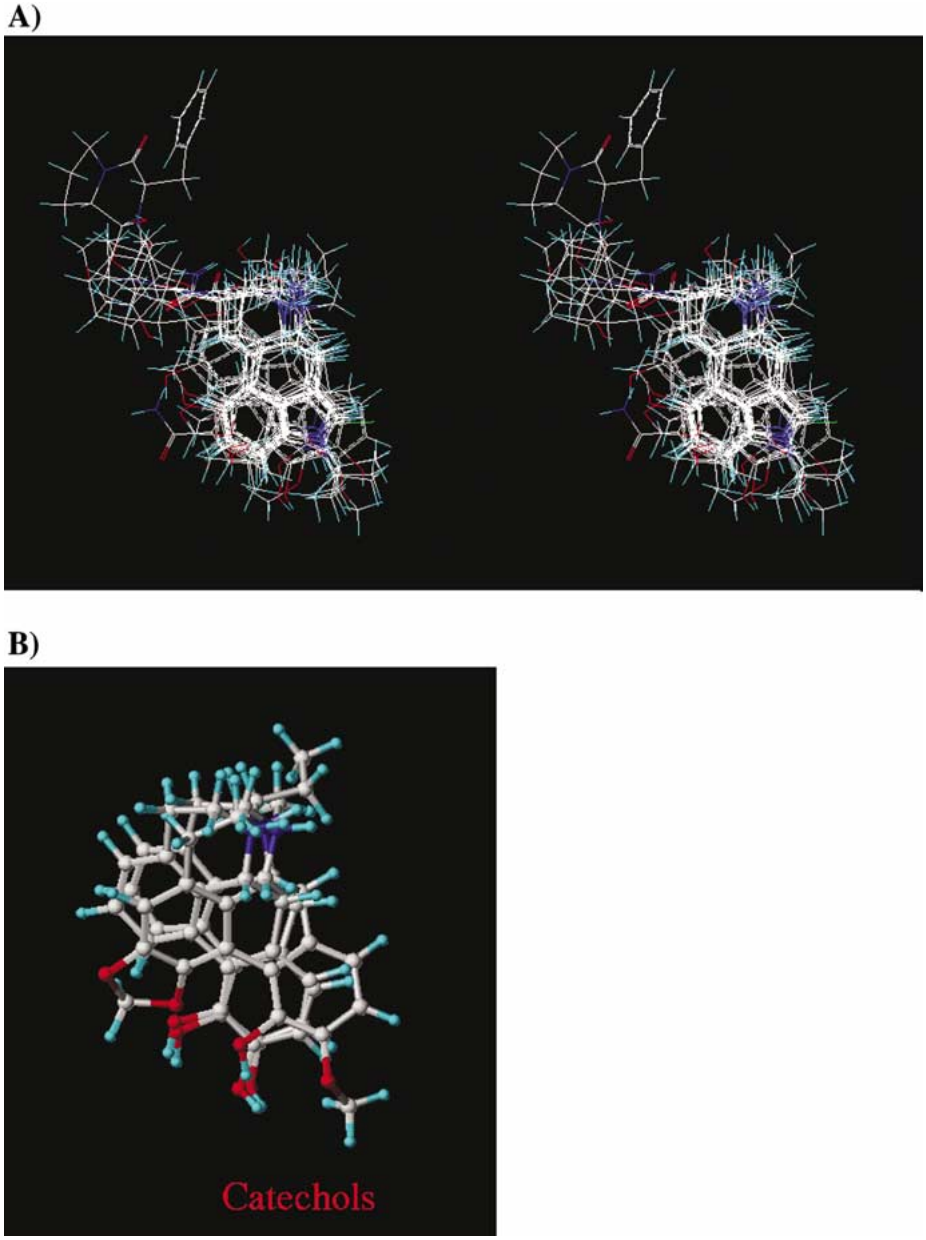

Figure 5. Alignment of compounds in the training set. (A) Stereo view of all compounds in the training set. (B) Stereo view of catechol-like compounds. (C) Stereo view of ergoline compounds. (D) Stereo view of indole-like compounds.

possible with a reasonable energy. Therefore, 5-CT was less suitable as a CoMFA template than lisuride.

Distance information

A crucial aspect of drug binding to serotonin receptors is the formation of the electrostatic interaction between an Asp residue (probably in transmembrane region III of the receptor) and the positively charged nitrogen of the ligand [22]. A second essential feature of agonist binding consists of the interactions between hydroxyl- or other hydrogen bonding elements of the compound and various Ser or other residues (likely within transmembrane region V of the receptor) [23]. Serine residues appear to be particularly useful in the monoamine receptors as hydrogen donors or acceptors [22, 23]. Important features of an alignment rule in-

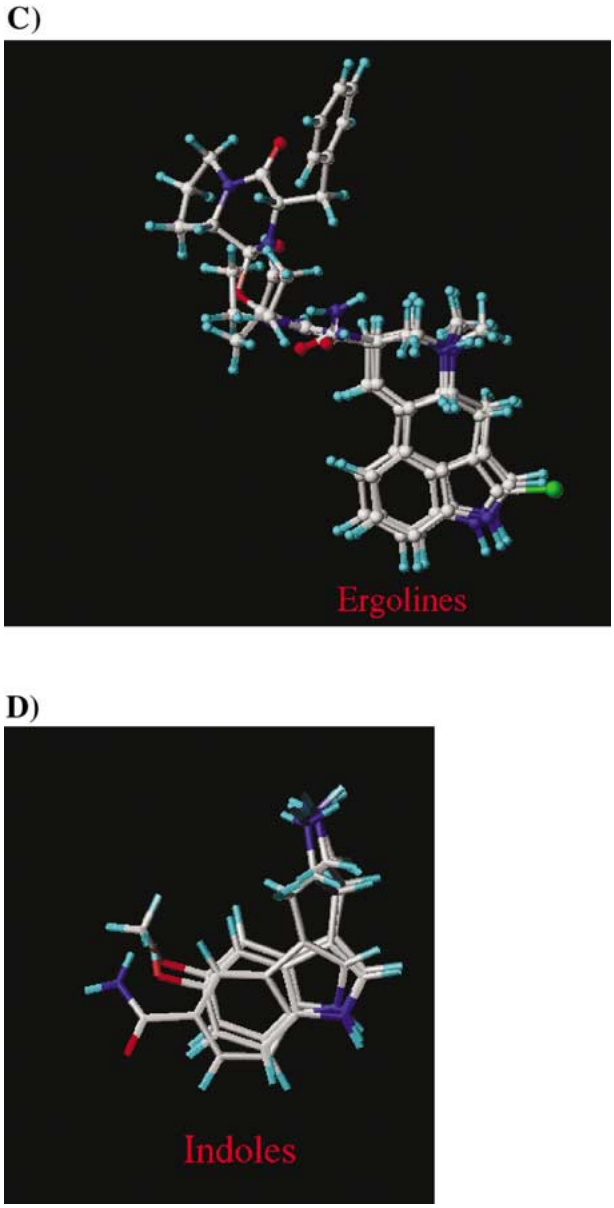

Figure 5. Continued.

clude the distances from the cationic nitrogen to the nitrogen (or other hydrogen binding moiety) of the indole ring, etc. An alignment rule was obtained from those structures having high affinity at the receptor (see Table 3; Figure 4). As previously discussed [2–4] such general features imply that certain portions of an agonist must be capable of electrostatic interactions and able to form hydrogen bonds to yield both high affinity and relative efficacy. CoMFA fields represent a portion of the enthalpic aspect of the overall free energy of the drug-receptor interaction. Also, the relationship between free energy and the equilibrium-binding constant is logarithmic. Thus, the affinity values given in μM were expressed as ln $(1/K_i)$.

Initial conformations and template selection

In the present study, SYBYL [21] v 6.6 was used for the modeling. Initial structures were generated as discussed above. As previously discussed [2–4] compounds are unlikely to bind to any receptor in their

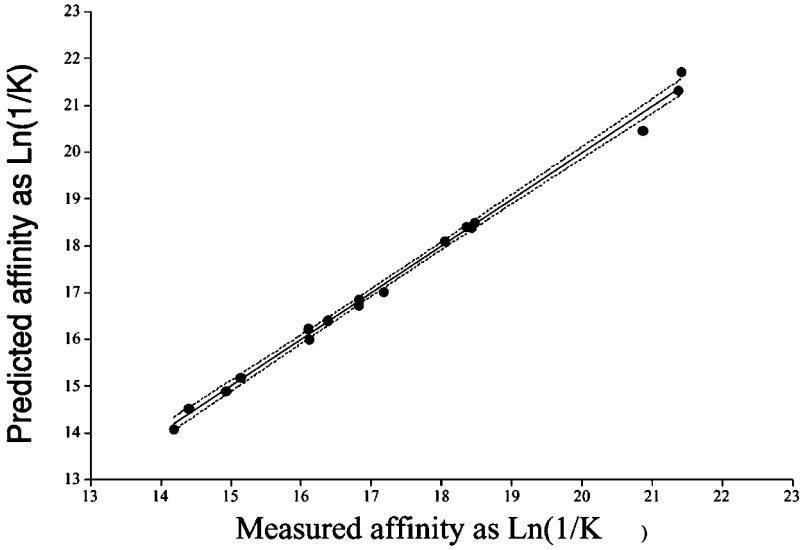

Figure 6. Correlation between measured and predicted affinities for training set compounds.

global minimum energy conformations. The reason is that some extent of torsional change or flexion of rotatable bonds is required to adapt the ligand and receptor to a complex of lower energy. Therefore, the so-called 'minimum' energy conformation resulting from a MAXIMIN2 procedure is only a useful starting point for possible candidate (binding) conformations of the compound. However, it is important to restrict the possible ligand conformations to those that are energetically accessible. Generally, a 10 kcal/mol cutoff value (difference between energies of the minimized and aligned conformers) is considered reasonable in CoMFA studies [24, 25]. Thus, energies of bound conformations did not exceed 10 kcal/mol above the 'minimum' calculated by the MAXIMIN2 procedure within SYBYL.

Alignment

Flexible field-fit protocols represent an improvement over 'static' fit methods for compound alignment. This is because they allow minor changes in compound conformation as a result of the field fit process [26]. Flexible field fits were done using the MAXIMIN2 procedure within Sybyl with the region set to that for the default CoMFA (for initial fits) and to the region associated with the best CoMFA (for subsequent fits). Steric and electrostatic fields extracted for the template compound (lisuride) were used in the fitting. AM1 charges were recalculated following the flexible field fit using the MOPAC procedure and the new conformational energy of the compound was obtained. The new charges were assigned and the compound replaced in the molecular data base. Following each flexible field-fit, the CoMFA model was derived using the SYBYL default parameters (see below).

Alternate compounds alignments

Amesergide was realigned using the flexible field fit procedures described above (Figures 7A and 7B). The energy of the compound was 45.3 kcal/mol (E_{min} = 42.3 kcal/mol). The alternate version of amesergide was substituted for the original version in the molecular spread sheet and autofill performed for the CoMFA. The q^2 was reduced slightly (from 0.851, shown in Table 4, to 0.833).

Similarly, laurolitsine was reoriented to make the other pair of hydroxyl groups available for hydrogen bonding to the receptor (Figures 7C and 7D), aligned with the template compound and substituted for the original version of laurolitsine. The energy of the compound was 15.8 kcal/mol (E_{min}, 7.6 kcal/mol). Substitution of the new version of laurolitsine and recalculation of the CoMFA/PLS lowered the q^2 to 0.705 (relative to the original 0.851).

CoMFA and partial least squares (PLS)

We have systematically investigated the effects of changing several CoMFA parameters, including dielectric (function of '1/r' vs. constant), grid step size (1.5, 2.0, 2.5 Å), probe atom type (H^+, O^-,

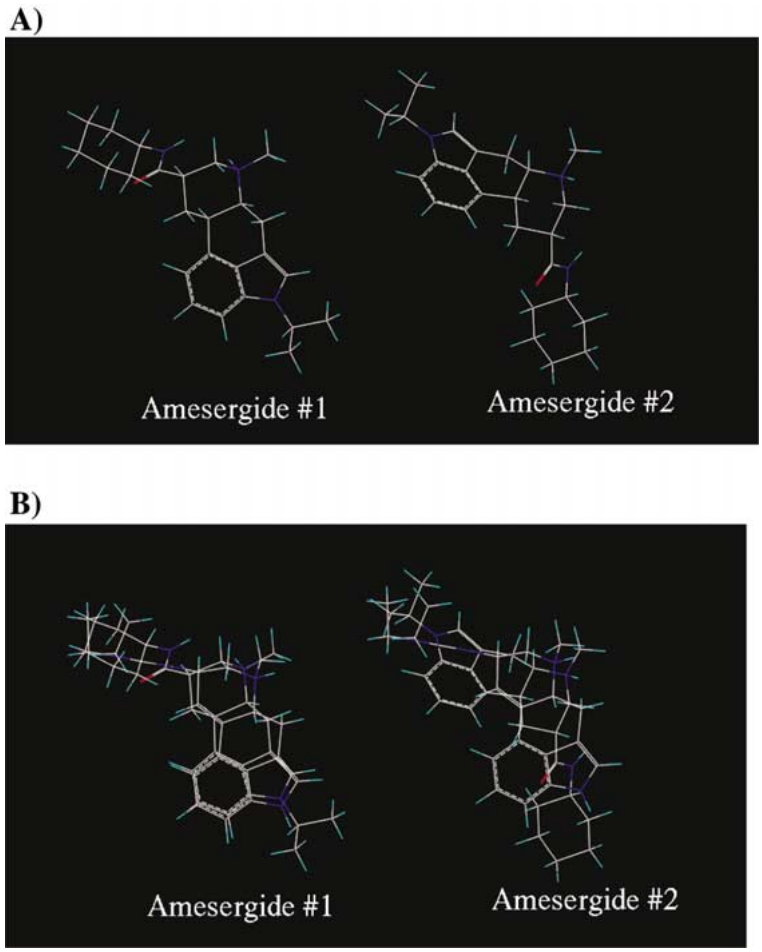

Figure 7. Alternate alignments of amesergide and laurolitsine. (A) Amesergide version #1 vs. amesergide version #2. (B) Amesergide + lisuride (template) version #1 vs. amesergide + lisuride version #2. (C) Laurolitsine version #1 vs. laurolitsine version #2. (D) Laurolitsine + lisuride (template) version #1 vs. laurolitsine + lisuride version #2.

C^{+}_{sp3}), and the column filtering values (from 1.0 to 4.0 kcal/mole in 0.5 kcal/mole increments). The initial cross-validation was performed using the 'leave one out' method.

Residual values for ln ($1/K_i$) represent the difference between the affinity predicted by the model vs. that measured. Training set compounds having high residuals were field-fit again and the CoMFA again determined. As described this is a 'manual-iterative' procedure in which the field-fit is refined based on improvement of the predictive validity of the CoMFA model until no further improvements are attainable [2–4].

PLS is a regression method that is useful in situations in which the number of predictor variables greatly exceeds the number of 'subjects' (compounds) [27]. As applied to computational chemistry, PLS provides an extremely useful strategy for inclusion of detailed information about the charge and bulk characteristics of biological molecules [26, 28–32]. PLS routinely incorporates thousands of predictor variables (as the steric and electrostatic interactions of a probe atom with each point in a 3D grid box) for a training set of compounds. Predictors are determined at the grid points of a 3-dimensional lattice (box) containing all members of the training set of aligned compounds. As in all regression methods, the PLS retains only

[1]In CoMFA, the probe atom interacts with each point in the 3D grid box. At some of those points no atoms can be found. At others, atoms are associated with training set compounds having low affinity. At still other grid points the probe atom would interact with atoms of compounds having high affinity. A variety of probe atom types are possible. The tetrahedral carbon with a positive charge is one of the most commonly used.

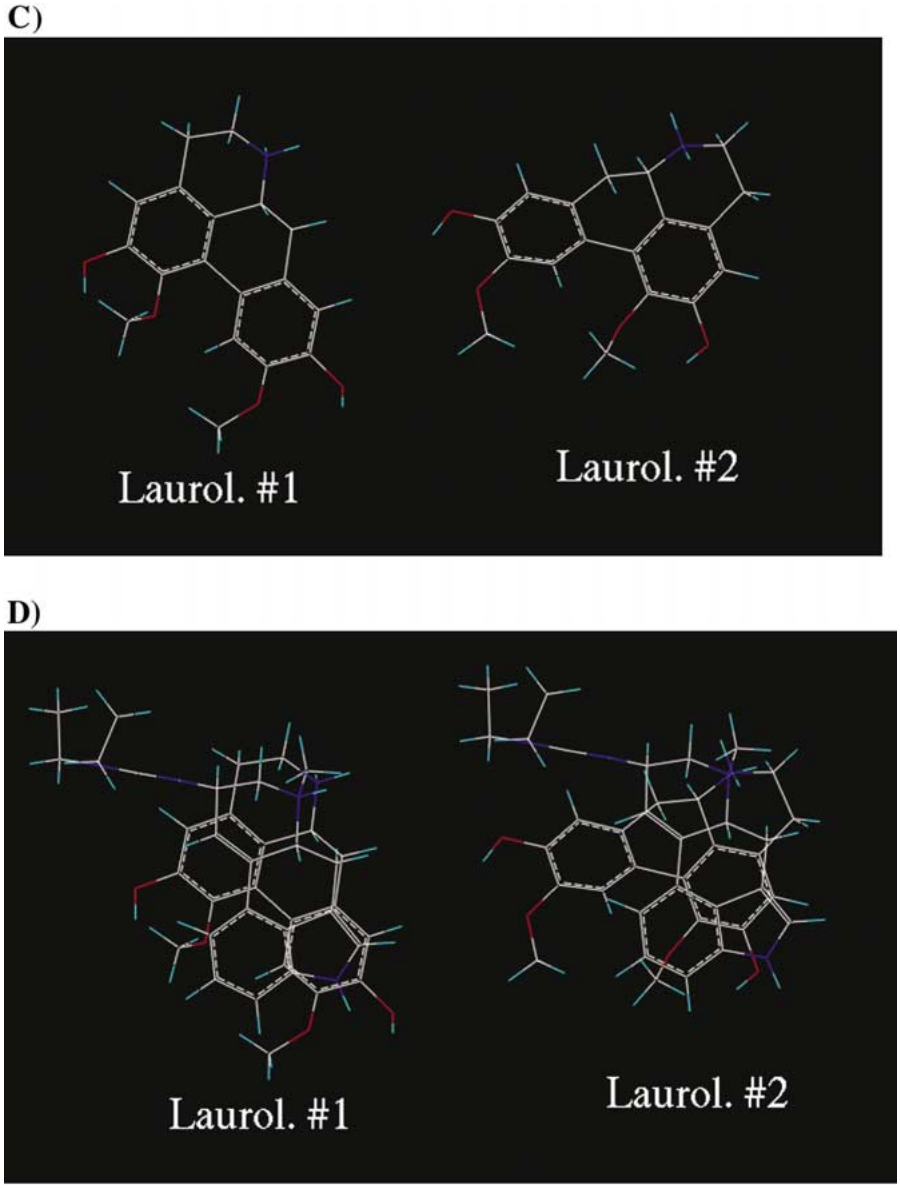

Figure 7. Continued.

those predictors in the final model that substantially account for the variance of the dependent variable (drug affinity). For example, the cationic nitrogen is clearly a necessary feature of drug binding to serotonin receptors. However, this feature has essentially no weight in the final CoMFA model because it is common to all training set compounds.

Region focusing, and CoMSIA

We tested the CoMFA using the Region Focus feature within SYBYL with the default SYBYL settings (discriminant function to the 0.3 power). This method uses a discriminant (or alternate) function to select those CoMFA components from an optimal non-cross-validated PLS analysis that contribute substantially to affinity prediction. Computational chemistry procedures for determining drug-receptor interactions only analyze a portion of the enthalpic aspects of bind-

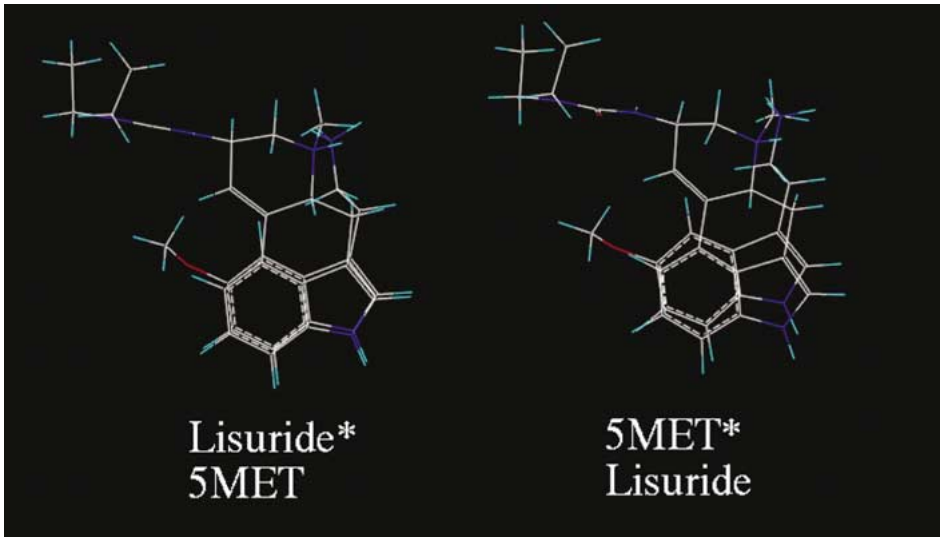

Figure 8. Alternate template for alignment (5-MET). Left: Original alignment: Lisuride (template)* + 5-MET aligned with it. Right: Alternate template: 5-MET (template)* + lisuride aligned with it.

ing. Other contributors to ligand binding, such as solvation, are ignored. However, a convenient first approximation of a portion of the solvation interaction may be done by incorporating hydrophobicity into the CoMFA model. We examined the effect of the hydrophobicity variable on the final model, by means of a variant of the standard hydrophobicity term derived from CoMSIA [4]. This feature was incorporated into the molecular spreadsheet.

Alternate template

We also tested the rigor of the CoMFA model by using a highly flexible compound as the template. 5-MET has the highest affinity of any compound in the training set (Table 1). However, it is highly flexible (Figure 8). For this reason, it would not normally be considered a likely candidate for a CoMFA template [32]. However, we chose the local minimum concentration for this compound. All other training set compounds were aligned with this alternate template and the CoMFA optimized as described above.

Prediction of affinities for a subset of training set compounds from a CoMFA model derived from the remaining compounds

Affinities for four of the training set compounds (amesergide, sergolexole, LY215840, and LY 53857) were derived from the literature [16]. Therefore, it was useful to attempt to demonstrate comparability of affinity measurements across laboratories by predicting affinities of these four compounds from a CoMFA model based on the remaining 13 compounds of the training set. Affinities were predicted using the predict property feature of the Sybyl molecular spreadsheet from the non-cross validated PLS analysis in two ways. First, we performed the PLS using only the 13 designated compounds but the original optimized CoMFA model. Second, we derived a new CoMFA/PLS analysis based entirely on the 13 remaining compounds.

3D-Search of chemical databases

One useful way to evaluate alignment rules associated with CoMFAs is to perform flexible 3D searches of large chemical databases for potential 'lead' compounds that possess the desired features [33]. Here, we used the UNITY software accessible through SYBYL to perform searches of the following databases: NCI, MDDR, ACD, CMC, and Maybridge [3, 20]. The query was a simple alignment rule representing distance between the cationic nitrogen, the hydrogen bonding group meta- to that nitrogen, and the C2 carbon of the aromatic ring. Distance constraints were based on the highest affinity ergoline compounds in the training set for these searches [3]. Subsequently, results from the searches (UNITY hit lists) were loaded into SYBYL molecular spreadsheets and a SYBYL similarity search performed with R-lisuride as the search template. This allowed a convenient rank

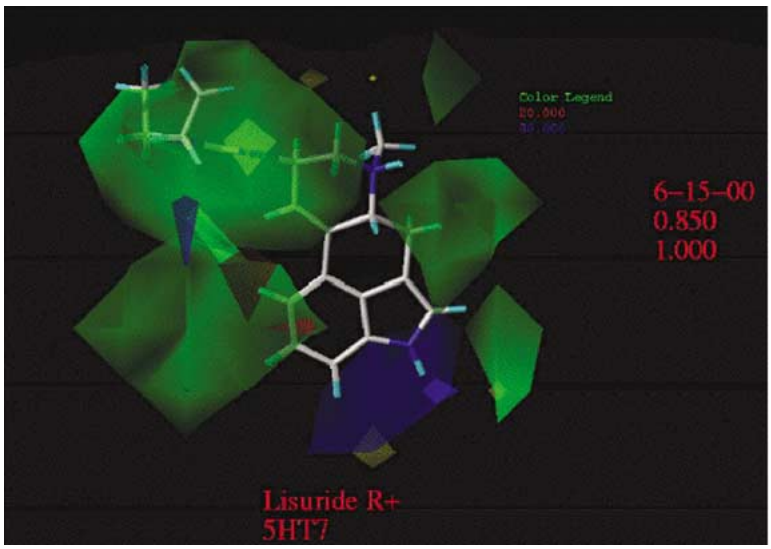

Figure 9. Contour map relating compound affinity at $5HT_7$ receptors to electrostatic and steric intermolecular interaction fields using a lisuride template. Positive electrostatic charge is favored (blue) or not favored (red) for high-affinity (80:20). Steric bulk is favored (green) or not favored (yellow) for high-affinity (80:20).

ordering of the compounds in the hit list based on their structural resemblance to lisuride.

Results

Drug affinity

We determined the affinity of 13 of the 17 training set compounds at $5HT_7$ receptors stably expressed in CHO cells as described using duplicate 10 point displacement curves against (3H)-5CT [7]. Competing ligands were run at approximately equal log intervals over approximately 5 orders of magnitude. Figure 2 shows data from a sample experiment for 5HT. Assays were performed under conditions that prevented coupling of the receptors to G proteins. Thus, Hill coefficients for competition binding curves did not differ significantly from unity (data not shown). Affinities of four additional training set compounds (amesurgide, LY215840, LY53857, sergolexole) were obtained from the literature [16]. Affinities of all 17 compounds are given in Table 1.

Adenylate cyclase activity

Figure 3A compares the ability of R- and S-8-OH-DPAT to elevate adenylate cyclase activity in membranes prepared from CHO cells heterologously expressing $5HT_7$ receptors. The R-isomer was approximately an order of magnitude more potent than the S-isomer of 8-OH-DPAT. The derived CoMFA model was successful in determining the affinity of the active isomer. The more active R-isomer (in terms of ability to elevate adenylate cyclase) had an EC50 of $\approx$ 130 nM vs. $\approx$1750 nM for the less active S-isomer (Figure 3A). Figure 3B compares the structures of the active R- and less active S-isomers of 8-OH-DPAT. The EC50 found in the present experiments is lower (higher potency) than those previously reported in the literature (Table 2). This may reflect, in part, the density of receptor expression or the coupling efficiency between receptor and signal transduction proteins derived from CHO cells.

Two-dimensional structures and training set compound alignment

We used flexible field fit procedures to determine the final alignments and conformations of training set compounds. The cationic nitrogen and hydrogen bonding regions were important features of the final alignment.

Alignment rule for $5HT_7$ receptor affinity

Figure 4 shows the alignment rule for binding of ligands to $5HT_7$ receptors. Panel A indicates the typical features, including the cationic nitrogen, hydrogen-bonding regions, and the centroid of the five-membered ring. The minimal height of the cationic

nitrogen above the plane of the five-membered ring is shown more clearly in Figure 4B of the same figure.

Table 3 shows the information derived from the alignment rule for the compounds of the final training set. R-lisuride was the template for the final CoMFA because of its structural similarity to other high-affinity compounds in the set, its relatively high-affinity at $5HT_7$ receptors, and its relative lack of conformational flexibility. The highest affinity compounds (5HT, 5-methoxytryptamine, and 5-CT) demonstrated a distance between the cationic nitrogen and the carbon of the five-member ring 'meta' to it of 5.8–6.0 Å. The height of the cationic nitrogen above the plane of the indole ring is another important alignment feature. The value for this element ranged from 0.4–1.0 Å for the high-affinity compounds at the $5HT_7$ receptor.

Ligand alignment via flexible field-fit

Figure 5 presents the alignment of the training set ligands. Figure 5A presents a stereo view of the entire training set. Figure 5B shows selected training set compounds having a catechol-like structure, Figure 5C shows compounds having the ergoline structure, while Figure 5D shows indole compounds. Taken together these four panels demonstrate the significant similarity of key binding features obtainable for compounds with extensive 2D-structural diversity.

Comparative Molecular Field Analysis/Partial Least Squares regression (PLS)

PLS incorporates as potential predictor variables the steric and electrostatic interactions of a probe atom at the grid points of a 3-dimensional lattice (box) containing all members of the training set of aligned compounds. PLS retains only those predictors in the final model that substantially account for the variance of the dependent variable (drug affinity). PLS methods specifically deal with common situations in computational chemistry in which there are thousands of predictor variables for a few compounds [28–31].

The final CoMFA model used both steric and electrostatic features. A steric cutoff of 15 and an electrostatic cutoff of 10 kcal/mol were used in the final model. The distance-dependent dielectric function yielded an improvement over models holding this value constant. The final CoMFA model utilized a Csp3+ probe atom, and a 2.0 Å step size. The SYBYL default region (within the grid box) was altered as described in Table 4 to improve the CoMFA model. The minimum σ value in the final model was 1.75 kcal/mole. Together, these parameters yielded an optimal final CoMFA model. Because these parameters were similar to those for previously generated CoMFA models for agonist affinity at dopamine receptors, they also facilitated comparisons among the models (see below) [34].

Table 5. Prediction of affinities of amesergide, sergolexole, LY215840, and LY53857 from the CoMFA model

Compound	Property	Value	CoMFA model
Amesurgide	Predicted	16.41	Optimized[a]
	Measured	16.37	Optimized
Sergolexole	Predicted	16.56	Optimized
	Measured	16.11	Optimized
LY215840	Predicted	16.47	Optimized
	Measured	18.04	Optimized
LY53857	Predicted	16.92	Optimized
	Measured	16.09	Optimized
Amesurgide	Predicted	16.11	Default[b]
	Measured	16.37	Default
Sergolexole	Predicted	16.15	Default
	Measured	16.11	Default
LY215840	Predicted	15.61	Default
	Measured	18.04	Default
LY53857	Predicted	16.40	Default
	Measured	16.09	Default

[a]Predicted using the CoMFA model from Table 4 with that CoMFA region. The PLS for 13 compounds remaining in the training set yielded a q^2 of 0.904 (5 principal components, SEP = 1.035, and 246/3024 columns used in the analysis).

[b]Predicted using a new CoMFA model based on the remaining 13 compounds of the training set. The PLS for 13 compounds remaining in the training set yielded a q^2 of 0.656 (5 principal components, SEP = 1.959, and 325/2772 columns used in the analysis).

The cross-validated r^2 (q^2) values that resulted from the various CoMFA options for ln ($1/K_i$) as the target property are given in Table 5. The optimal CoMFA/PLS run for the 17 compounds of the training set using the SYBYL default settings yielded a q^2 value of 0.851 with 5 principal components and a standard error of prediction (SEP) of 1.061. The PLS with 5 components using the no-validation option yielded an r^2 of 0.996 and a standard error of the mean (SEM) of 0.183 with steric features of the model accounting for 41% and electrostatic features accounting for 59% of the variance in the dependent variable.

Region Focusing within SYBYL was conducted on the optimal non-cross validated CoMFA model. This protocol includes only those features of the CoMFA

that optimally contribute to the model. As expected, an examination of Table 4 shows that the number of CoMFA columns used in the model resulting from Region Focusing was somewhat smaller than the number of columns used in the original optimal model (112 of 3024 vs. 274 of 3024). Region focusing (using the default setting) slightly worsened the q^2 to 0.808 (with 6 principal components and a SEP of 1.265).

Figure 6 shows the relationships between measured and predicted affinities for the optimum CoMFA model. Two of the training set compounds had predicted affinities outside the 95% confidence intervals. They were 5HT and 5MET. An initial estimate of a possible entropic contribution to drug binding was made using a hydrophobic term added as a component of a CoMSIA along with the steric and electrostatic and donor and acceptor atoms (within SYBYL 6.6). This resulted in a PLS in which $5HT_7$ affinity was predicted by a combination of five terms: electrostatics, steric features, hydrophobics, donor atom characteristics, and acceptor atom characteristics. As shown in Table 4, use of these CoMSIA features (at default settings) resulted in a q^2 value of 0.856 (6 principal components, an SEP of 1.096, and use of 1021 out of 7560 columns in the analysis).

Alternative compound alignments

We explored alternative alignments for two compounds for which the alternative binding modes seemed most reasonable. First, we utilized a different alignment for amesergide to allow the third nitrogen to serve as a hydrogen bonding moiety. Figure 7A compares the orientations for amesergide in the original and alternative alignments. Figure 7B shows amesergide in relation to the template compound (lisuride). Amesergide was aligned using the flexible field fit procedures described above. The energy of the compound was 45.3 kcal/mol (E_{min} = 42.3 kcal/mol). The alternate version of amesergide was substituted for the original version in the molecular spread sheet and autofill performed for the CoMFA. The q^2 was reduced slightly (from 0.851, shown in Table 4, to 0.833).

Similarly, laurolitsine was reoriented to make the other pair of hydroxyl groups available for hydrogen bonding to the receptor (Figures 7C and 7D), aligned with the template compound and substituted for the original version of laurolitsine. The energy of the compound was 15.8 kcal/mol (E_{min}, 7.6 kcal/mol). Substitution of the new version of laurolitsine and recalculation of the CoMFA/PLS lowered the q^2 to 0.705 (relative to the original 0.851).

Alternate template

We used the high affinity compound 5-MET as an alternate template for the CoMFA. We selected the local minimum energy conformation as the template conformation of this compound. Other CoMFA/PLS procedures were done as with the original model using lisuride as the template. Using the default Sybyl parameters, we obtained a q^2 of 0.804 (with 5 principal components, an SEP value of 1.216, and incorporation of 362 of 3024 columns into the model). Thus, the data suggest that it may be useful to use the highest affinity compound in the training set as an alternate template for compound alignment.

Prediction of affinities

Prediction of affinities was done for a subset of training set compounds from a CoMFA model derived from the remaining compounds. Affinities for four of the training set compounds (amesergide, sergolexole, LY215840, and LY 53857) were derived from the literature [16]. We evaluated the comparability of affinity measurements across laboratories by predicting affinities of these four compounds from a CoMFA model based on the remaining 13 compounds of the training set. Affinities were predicted using the predict property feature of the SYBYL molecular spreadsheet from the non-cross validated PLS analysis in two ways. First, we performed the PLS using only the 13 designated compounds but the original optimized CoMFA model. Second, we derived a new CoMFA/PLS based entirely on the 13 remaining compounds. These results are summarized in Table 5. Using a PLS derived from the original CoMFA model, prediction of affinity was extremely good for amesergide, sergolexole, and LY53857 (<0.5 log unit). Prediction was not as good for LY215840 (measured affinity was 18.04 vs. predicted affinity of 16.47 Ln units). Similarly, another set of predictions for affinities of the same compounds was derived from a new CoMFA model based on just the 13 remaining compounds of the training set. Once again, predictions were excellent for 3 of the 4 compounds and less good for LY215840. Overall, the results indicate that measurement of drug affinity across laboratories was consistent.

Contour map

Figure 9, shows the contour map of the final $5HT_7$ CoMFA model. Both steric (80:20 as favored: unfavored) and electrostatic (80:20) fields were utilized, since this improved the standard error of prediction (SEP) and the q^2 value over alternative models. The contour map showed several potentially important characteristics. First, it exhibited little in the way of electrostatic features in the vicinity of the cationic nitrogen. This is consistent with the idea that differences among the training set compounds in this region of the molecule are not of major importance in high affinity binding. This is consistent with the importance of the electrostatic bond between the N+ and an Asp (likely within transmembrane region III) in binding of all $5HT_7$ ligands [22]. Steric features near the cationic nitrogen are of some importance in differentiating ligand binding affinity, particularly sterically favored regions.

A second salient characteristic is that hydrogen-bonding regions are highly significant predictors of high affinity for $5HT_7$ receptor ligands. The regions in which positive charge is favored include the vicinity of the hydrogen-bonding nitrogen and the regions near both the five- and six-membered rings. Steric features, especially where steric bulk is favored for high affinity, appear prominently in the model, particularly a sterically favored region that lies close to the cationic nitrogen.

Figure 10A–E, shows the contour map with acceptor, donor, electrostatic, steric, and hydrophobicity components resulting from a CoMSIA for the training set. Here, the PLS was run using the hydrophobic, steric/electrostatic, and donor/acceptor CoMFA columns as independent variables with Ln (1/Kd) as the dependent variable. All contours are shown as favored: unfavored. A simple interpretation of this contour map is that the hydrophobically favored regions represent those portions of the ligand that are least exposed to the surface of the receptor during binding. A comparison of panels A and B in this figure indicates that hydrophobicity complements positive electrostatic charge in yielding information about likely hydrogen bonding regions of the receptor active site that interact most favorably with the ligand. Specifically, it appears that the alkyl extension of the lisuride template molecule is associated with an electrostatically favored region (blue region in the upper left portion of Figure 10C). This site may be positioned in relation to the active site of the $5HT_7$ receptor by the presence of the hydrophobically-favored (orange region in the upper left portion of Figure 10E) portion of the molecule. More generally, those regions in Figure 10E in which hydrophobicity is not favored for high-affinity binding (white in Figure 10E) serve to define the regions in which positive charge favors high-affinity (blue in Figure 10C). Additional hydrophobic capacity favored (orange in Figure 10E) and not favored (white in Figure 10E) in some of the regions in which steric bulk favors high-affinity binding (green in Figure 10D) further served to refine the steric features of the model. Qualitative (contour map) aspects of the CoMFA model for high affinity binding at the $5HT_7$ receptor appear to be enhanced by the addition of a hydrophobic component.

Table 6. Cross-validation analysis results for CoMFA model from Table 4 at recombinant $5HT_7$ receptors

Cross-validation run # (5 groups)	q^2	# principal components	Standard error of prediction
1	0.734	4	1.358
2	0.866	4	0.964
3	0.669	4	1.515
4	0.741	3	1.287
5	0.818	4	1.122
6	0.847	6	1.127
7	0.707	4	1.426
8	0.717	4	1.399
9	0.736	4	1.352
10	0.748	5	1.380
11	0.867	5	1.002
12	0.836	4	1.066
13	0.738	4	1.348
14	0.734	6	1.487
15	0.724	4	1.383
16	0.814	5	1.187
17	0.860	4	0.984
18	0.848	5	1.073
19	0.854	4	1.007
20	0.724	6	1.514

PLS cross-validations runs were done using the optimum model from Table 4. This model had a steric cutoff of 15 and an electrostatic cutoff of 10 kcal/mol. The model also employed a minimum sigma of 1.75 Å, a step size of 2.0 Å, a dielectric equal to 1/r, and a Csp3+ probe atom. The model used a CoMFA grid box with coordinates X (−13.79, 8.54), Y (−10.58, 16.15), and Z (−12.44, 5.45) with a total of 3024 possible CoMFA columns.

Evaluation of the CoMFA model

To evaluate the optimum CoMFA model, a series of 20 cross-validations was runs using groups of 5 per run. Results are summarized in Table 6. The mean q^2 was

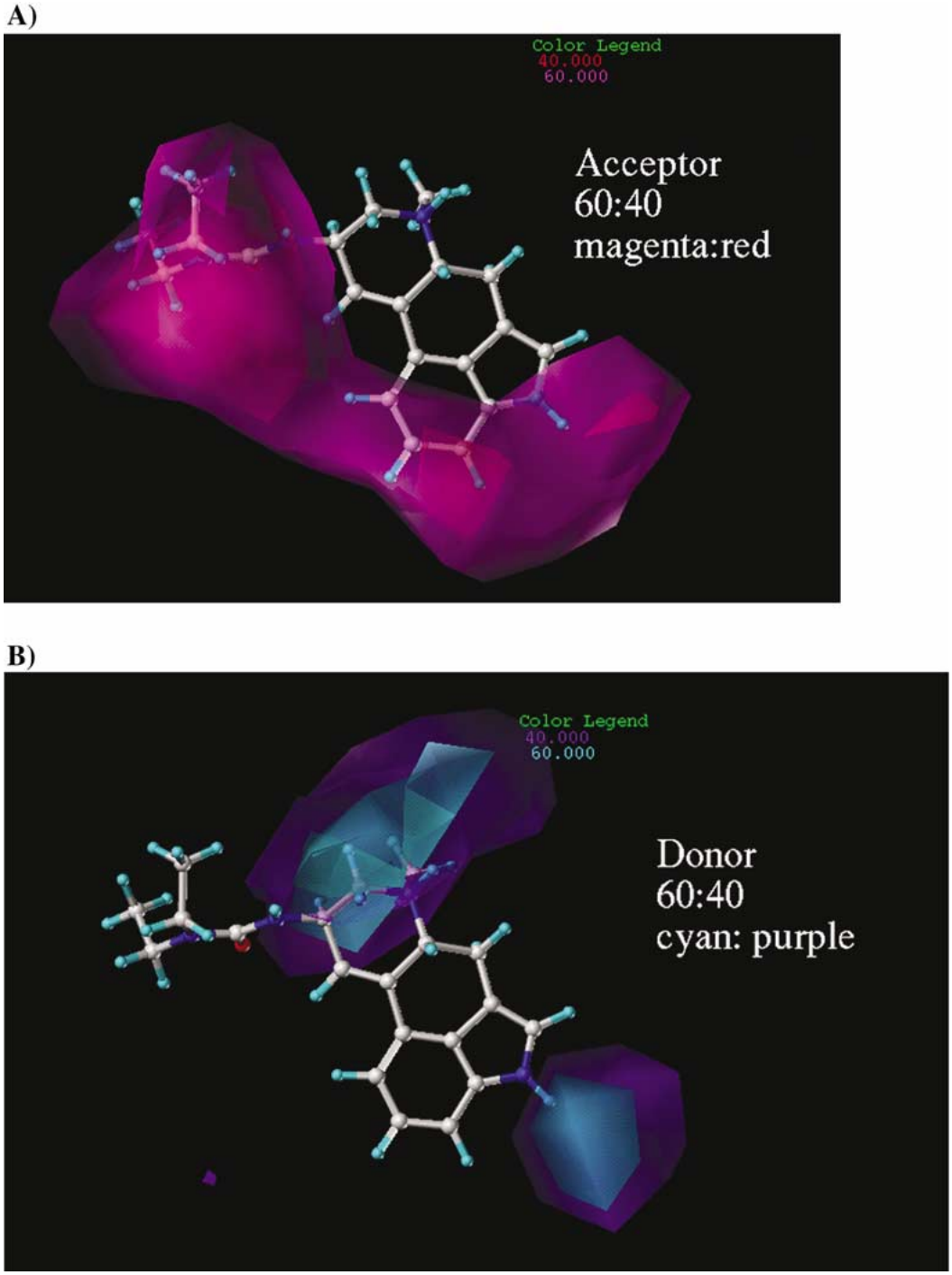

Figure 10. CoMSIA contour maps. Acceptor sites: Favored = magenta; unfavored = red (60:40). Donor sites: Favored = cyan; unfavored = purple (60:40). Electrostatic: Favored = blue; unfavored = red (60:40). Steric: Favored = green; unfavored = yellow (60:40). Hydrophobic: Favored = orange; unfavored = white (60:40).

C)

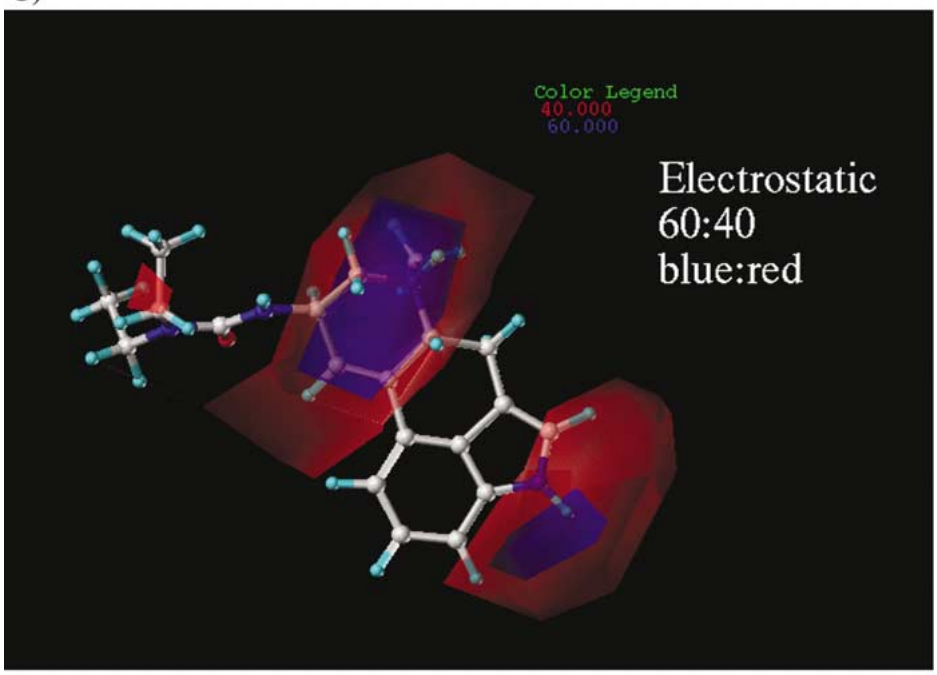

D)

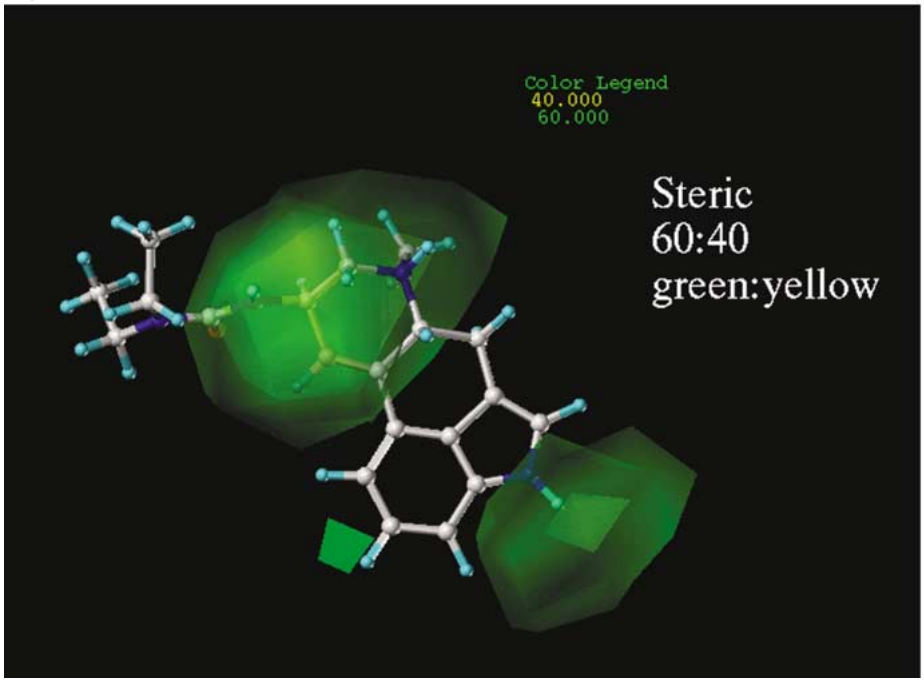

Figure 10. Continued.

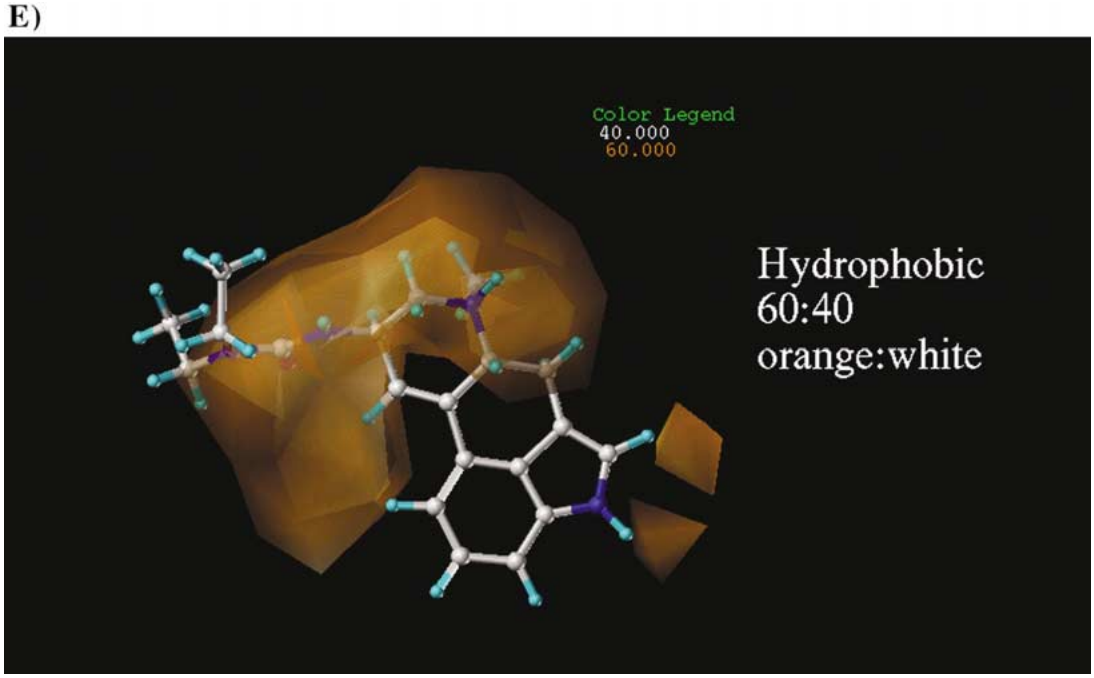

Figure 10. Continued.

0.779 ± 0.015 with a range from 0.669 to 0.867. The mean SEP for the 20 runs was 1.249 ± 0.043 with a range from 0.964 to 1.515. Thus, the present model is robust enough to predict ligand affinity at $5HT_7$ receptors even when using information from only 12 of the 17 compounds in the training set.

3D-chemical data base search and similarity index

Intially, the validity of the query (Figure 11A) was tested by applying it to the training set. The 'hits' from the search included all four of the highest affinity compounds of the training set (5-MET, 5-CT, 5HT, and lisuride) and excluded four of the lowest affinity compounds (apomorphine, bulbocapnine, laurolitsine, and NPA).

Table 7 summarizes the results from searching five 3D-chemical databases via the UNITY program accessible within SYBYL [3] with a simple search query derived from the alignment rule for the $5HT_7$ receptor. Figure 7A shows the search query. In all instances a significant reduction in the number of compounds (Table 6, column 2 vs. column 3) was obtained while all database searches yielded at least two hits. Thus, a simple 3D search query yields a reasonable number of potential lead compounds for the discovery of novel $5HT_7$ receptor ligands. Refining the search query using an exclusion volume derived from the CoMFA contour map can be used to further refine the hit lists resulting from the search.

Similarity indices were calculated for the compounds in each hit list by using the similarity index features within the SYBYL molecular spreadsheet subroutine (Table 7, column 4). Here, the reference compound for the ranking was the template, R-lisuride. In most cases, the compounds yielded modest similarity to lisuride (in the range of 0.5 on

Table 7. 3D-chemical database search results for ligands at recombinant $5HT_7$ receptors[a]

Database	Compounds	Hits	Similarity
Maybridge	61184	9	0.49
ACD	201540	51	0.52
CMC	7100	2	0.45
MDDR	90158	38	0.79, 0.74[b]
NCI	117649	84	0.50

[a]The 3D-searches were based on a preliminary CoMFA model without 8-OH-DPAT and terguride.
[b]Search of this database yielded compounds #148982 and #147760.

[2]The 3D-searches were done using an earlier version of the CoMFA model with 15 ligands (8-OH-DPAT and terguride were not included).

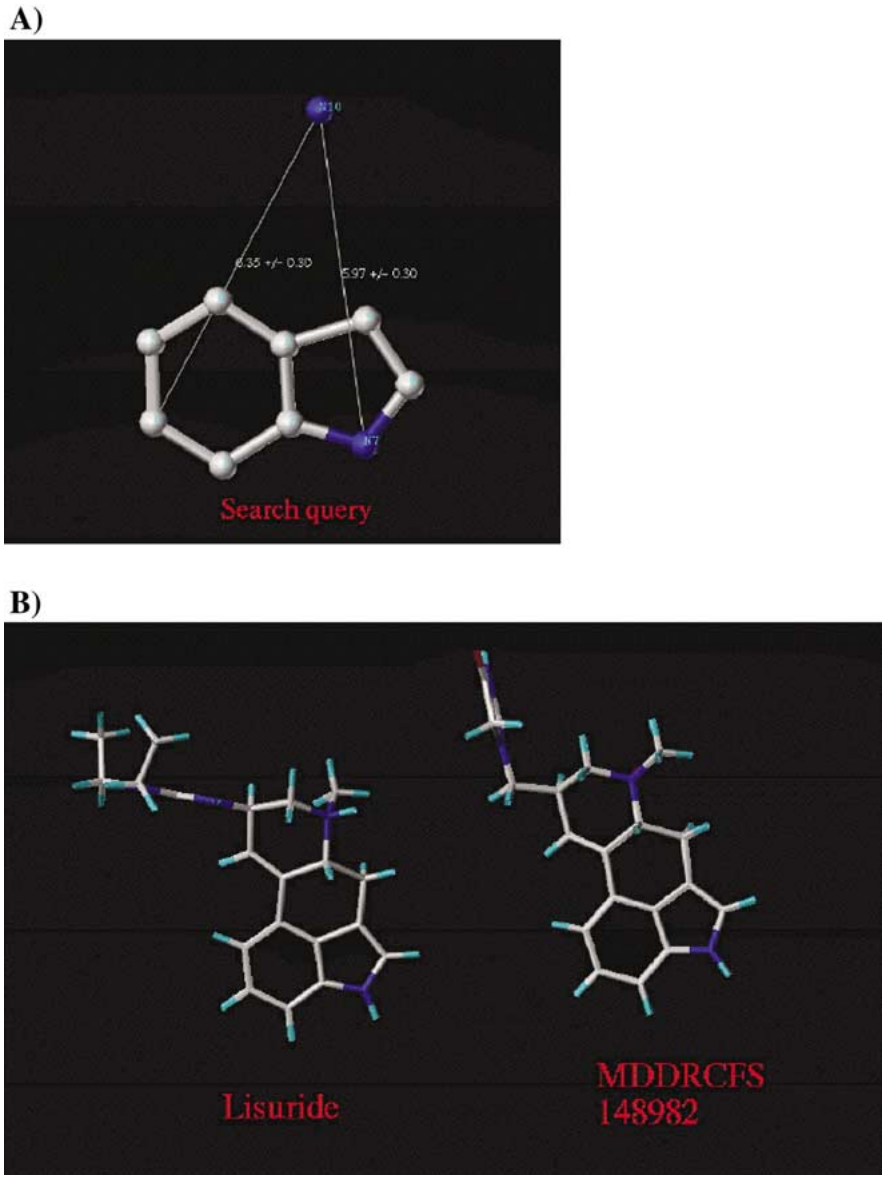

Figure 11. 3D-chemical database search results. (A) Search query. (B) Template for similarity search (lisuride) vs. compound with similarity index value of 0.79. (C) Two compounds having the highest similarity to the template.

a 0–1.0 scale). However, one compound of interest was identified as a result of searching the hit list derived from the MDDR database. This compound had a similarity index of 0.79 (compound #148982; Figure 11B) compared to lisuride. A second compound (#147760) had a similarity index of 0.74 relative to lisuride. These two compounds are depicted together in Figure 11C. Compound #148982 was identified as 1-(6-Methyl-9-ergolen-8-beta-y-l-methyl)-imidazolidine-2, 4-dione N6-oxide. Compound #147760 was identified as 1-(6-Methyl-9-ergolen-8-beta-y-l-methyl)-pyrimidine-2, 4(1H,3H)-dione N6-oxide. The source for both compounds was Farmitalia Carlo Erba. Both compounds were indicated to have anti-hypertensive activity.

Comparison with other CoMFA models

We have previously reported CoMFA models for G-protein coupled dopamine receptors positively (D_1, [2, 3]) and negatively (D_2, [3, 4]) linked to adenylate

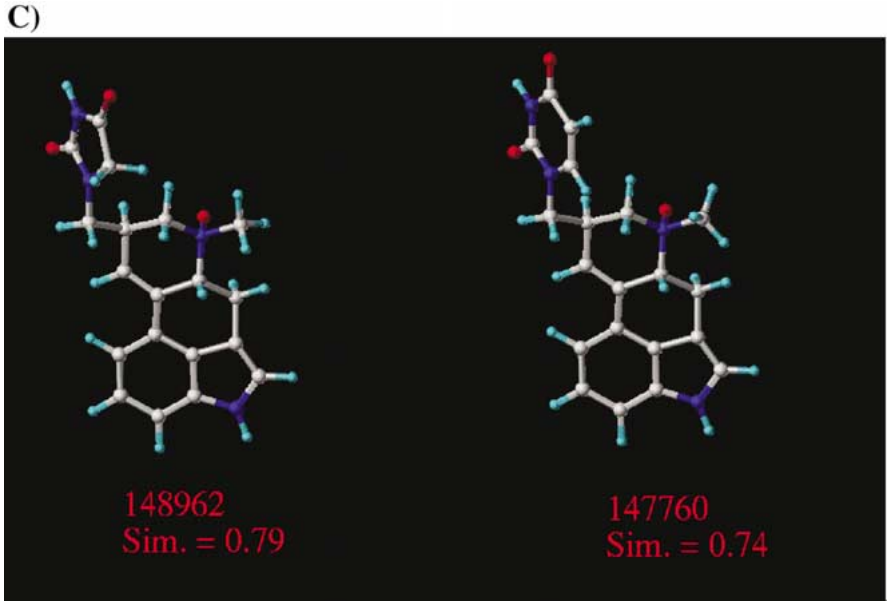

Figure 11. Continued.

cyclase. The models shown were obtained under conditions virtually identical to that for the present $5HT_7$ model. This facilitates a comparison among them.

Figure 12 presents contour maps for D_1 and D_2 receptors. All are shown with 80:20 (favored:unfavored) to facilitate comparisons among them. The current $5HT_7$ contour map (Figure 12A, the same contour as Figure 9 but slightly rotated) and the D_1 map (Figure 12B) are similar. Similarities are most marked in the presence of positive charge being favored near the hydrogen bonding regions of the molecule and in the general significance of steric aspects of the intermolecular interactions. However, the $5HT_7$ contour map differs from that for the D_1 dopamine receptor. For the former, steric bulk is highly favored over most regions of the receptor for high-affinity drug-receptor interactions, whereas for the D_1 receptor steric bulk is generally not favored [2, 3].

Comparing the contour maps for the D_2 dopamine receptor (Figure 12C) with that for the $5HT_7$ receptor, a similarity is that positive charge is highly favored near the hydrogen-bonding region for both models. However, the D_2 model has a second large region at the opposite end of the binding pocket in which positive charge is also favored, while the $5HT_7$ model does not. Sterically, the two models are dramatically different from one another. Thus, the $5HT_7$ model contains a large spatial region in which steric bulk is favored for high affinity binding while the D_2 model generally is unfavorable for high-affinity in the same relative position. [3, 4]

[3]The images used in this figure were generated for the present paper from the data used to generate Figures 5 and 6 in Wilcox et al. [3] CoMFA-based prediction of agonist affinities at recombinant D1 vs. D2 dopamine receptors.

Discussion

Data shown in Figure 3 represent the first report of the potency and intrinsic activity of the resolved isomers of the 5HT receptor agonist, 8-OH-DPAT. As indicated in Table 3, the information on the racemate suggests that this compound is a potent partial agonist at $5HT_7$ receptors as well as $5HT_{1A}$ receptors (pKa 8.2) [35]. The fact that the potency is comparable at $5HT_7$ and $5HT_{1A}$ receptors (present results and [7]) suggests a role for $5HT_7$ receptors in many of the behavioral actions of 8-OH-DPAT. One of the highest affinity compounds in the training set is 5-CT. This drug exhibits high affinity for members of the $5HT_1$ subfamily, but markedly lower affinity for the $5HT_2$, $5HT_3$, and $5HT_4$ receptor subfamilies [35]. These results suggest that the $5HT_{1A}$ receptor (negatively coupled to adenylate cyclase) and the $5HT_7$ receptor (positively coupled to the enzyme) share key features for agonist binding [34]. Further support for the similarity in active sites for the $5HT_{1A}$ and $5HT_7$ receptors is provided below.

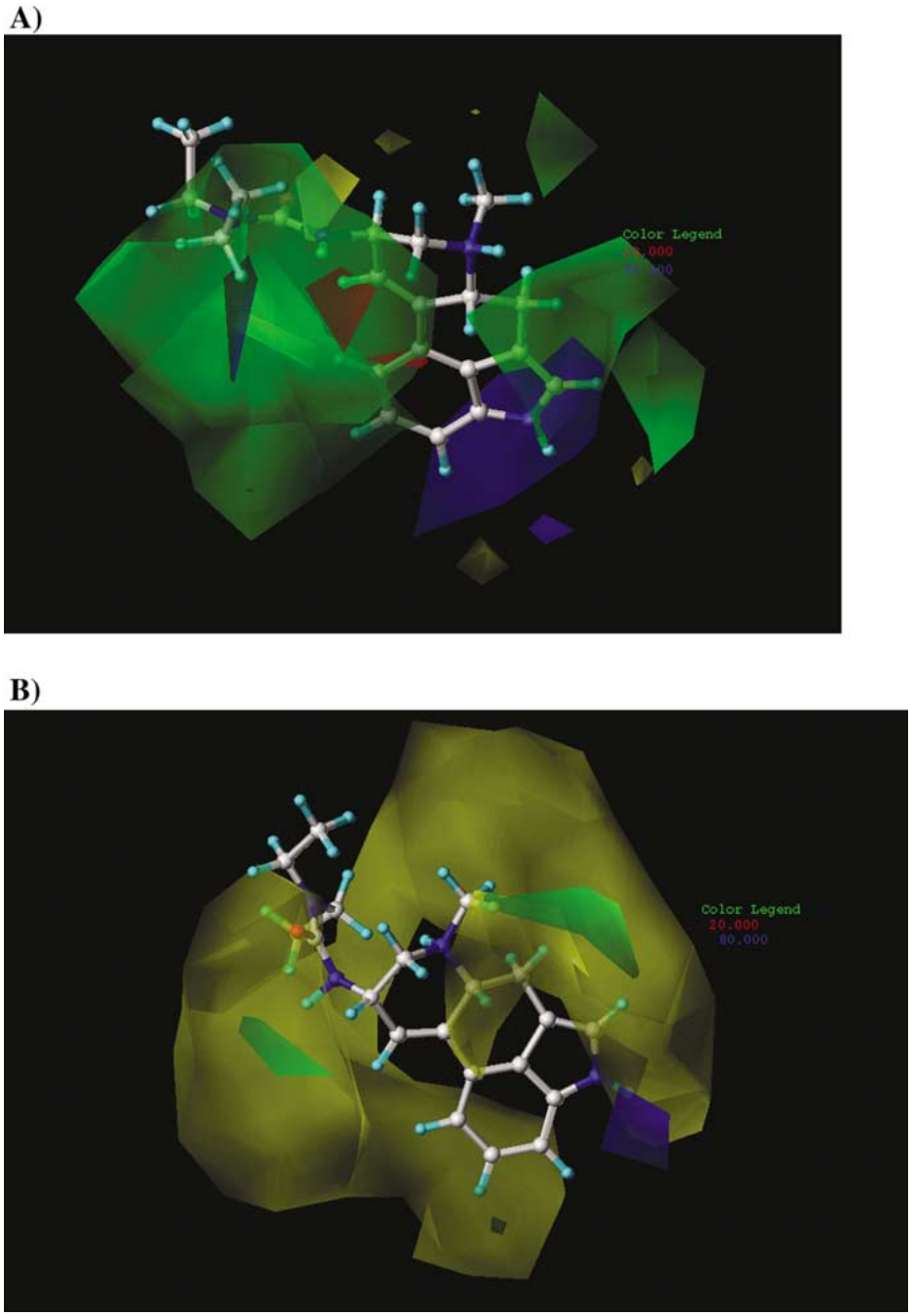

Figure 12. Contour maps relating compound affinity at $5HT_7$ (A), D_1 dopamine (B) and D_2 (C) dopamine receptors to electrostatic and steric intermolecular interaction fields. (A) $5HT_7$ receptor model – lisuride template. R-lisuride is shown in the figure. Positive electrostatic charge is favored (blue) or not favored (red) for high-affinity (80:20). Steric bulk is favored (green) or not favored (yellow) for high-affinity (80:20). (This figure is rotated from that shown in Figure 9.) (B) D_1 dopamine receptor model – Br-APB template. R-lisuride is shown in the figure. Positive electrostatic charge is favored (blue) or not favored (red) for high-affinity (80:20). Steric bulk is favored (green) or not favored (yellow) for high-affinity (80:20). (C) D_2 dopamine receptor model – Bromocriptine template. R-lisuride is shown in the figure. Positive electrostatic charge is favored (blue) or not favored (red) for high-affinity (80:20). Steric bulk is favored (green) or not favored (yellow) for high-affinity (80:20).

C)

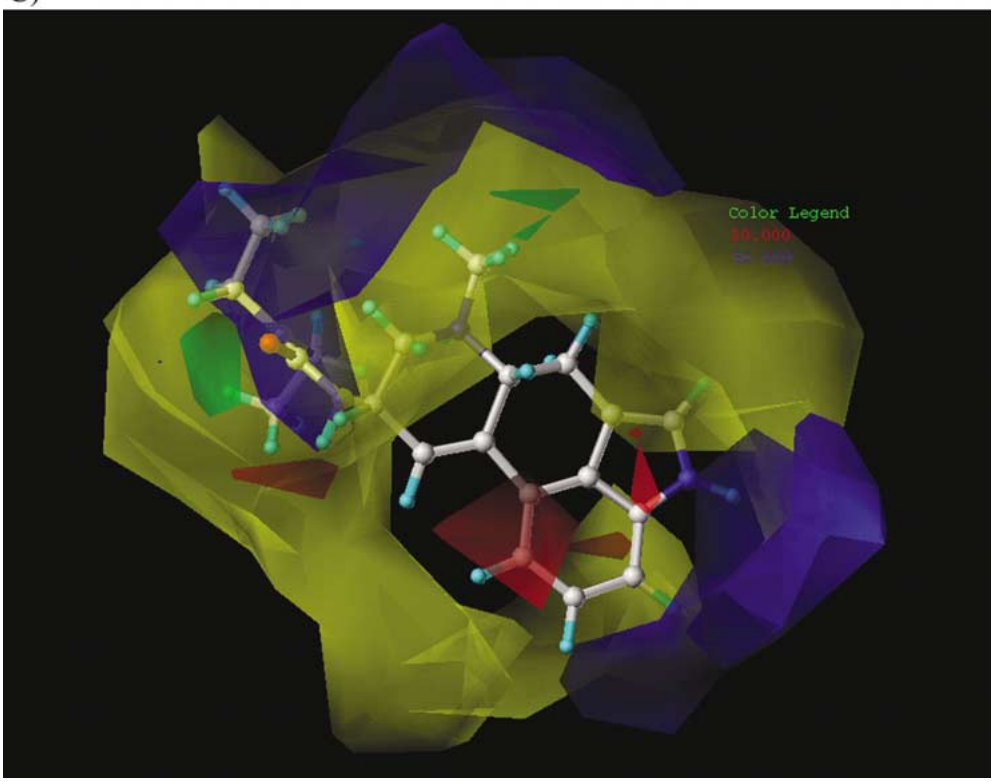

Figure 12. Continued.

The present results add to the information on interactions of ligands with G protein coupled receptors obtained through computational chemistry methods [2–4, 22, 26, 36]. Here, we determined the extent to which CoMFA-derived models of the $5HT_7$ receptor could usefully predict affinity for a highly diverse set of ligands. Using a series of 20 cross-validation runs with groups of 5 compounds to evaluate the CoMFA model we found that the mean q^2 was 0.779 ± 0.015 with a mean SEP of 1.249 ± 0.043. Thus, the overall model can predict affinity of sets of 5 training set ligands using only the information from 12 of the 17 compounds in the $5HT_7$ training set.

The contour map derived from the CoMFA model illustrated several potentially important aspects of drug interactions at $5HT_7$ receptors. As with other recent CoMFA models for D_1 and D_2 dopamine receptors [2–4] steric features near the cationic nitrogen are of some importance in differentiating ligand-binding affinity for the $5HT_7$ receptor. A second important characteristic is that regions in which positive charge is favored include the vicinity of the hydrogen-bonding nitrogen, and the regions near the five- and six-membered rings. Steric features, especially regions in which steric bulk is favored for high affinity, appear prominently in the $5HT_7$ model. Consistent with what we recently observed for the D_2 dopamine receptor [4], addition of a hydrophobic component slightly worsened the $5HT_7$ model. This suggested a potentially important role for this factor in positioning the alkyl side chain of the highest affinity compounds properly in the receptor active site.

There are a number of papers modeling the interactions of drugs with various 5HT receptors (see [22] for review). Wishart et al. [22] noted that the 1994 model of Kuipers [37] was able to account for the high-affinity of 8-OH-DPAT to the $5HT_{1A}$ receptor as well as its relative selectivity for that receptor vs. those of the $5HT_2$ subfamily. As expected, the Kuipers [37] model favored a three point binding interaction between the cationic nitrogen of the drug and the Asp of transmembrane helix III. The investigators also suggested that two hydrogen bonds were formed between the drug and a Ser and Thr of helix V. The authors further suggested that the ability of one of the bulky n-propyl groups of 8-OH-DPAT to form hydrophobic

interactions with residues in helices III and IV of the $5HT_{1A}$ receptor that were not accessible to the drug at the $5HT_2$ receptors may have provided part of the basis for selectivity. This result implies that the $5HT_7$ receptor should also have homologous residues located in helices III and IV. Indeed, a preliminary examination of the 2D structure of the $5HT_7$ receptor suggests that appropriate residues are well positioned in helices III and IV. It will be important to develop a protein homology model for the $5HT_7$ receptor to determine the extent to which this is actually possible.

Based also on the high affinity of 8-OH-DPAT for $5HT_{1A}$ and $5HT_7$ receptors, it may be reasonable to extrapolate from some mutagenesis data obtained for the $5HT_{1A}$ receptor to the $5HT_7$. It was proposed that Asn396 and Ser393 of the rat $5HT_{1A}$ receptor played an important role in the selective affinity of 8-OH-DPAT because mutations at either residue reduced drug affinity [38]. Accordingly, it is predicted that homologous residues in the guinea pig $5HT_7$ receptor would also be exposed to the surface of the binding pocket and in a position to influence agonist binding. The guinea pig $5HT_7$ receptor (present study) has an Asn in position 389 that seems suitable (homologous to the rat Asn 396). The receptor also has three Ser residues at positions 360, 378, and 398, which also might fulfill the same role as the Ser 393 in the rat $5HT_{1A}$ receptor [39, 40].

The CoMFA model derived here for affinity at the $5HT_7$ receptor provided a useful basis for developing a simple search query for probing 3D chemical databases. Limited numbers of hits from each database were obtained which were easily rank ordered using the similarity index feature present in SYBYL molecular spreadsheets. Two compounds with high similarity to the template compound and, thus, with significant potential as $5HT_7$ receptor ligands were discovered with this procedure. This result offers exciting possibilities for data-mining new ligands for this important receptor.

It was of interest that the 3D-search/similarity index procedures yielded two compounds with marked structural similarity to the template R-lisuride. Lisuride has high affinity for receptors of the D_2 dopamine subfamily and is a Parkinson's disease drug [3, 34, 41]. This suggests that the identified agents may also have some affinity for dopamine receptors. The fact that the two potential lead compounds were identified as anti-hypertensive agents is intriguing. The $5HT_7$ receptors are expressed in the coronary arteries and systemic capillary beds as well as in brain areas regulating vascular functions [1, 16, 42, 43]. Generally, compounds having the tetracyclic ergoline skeleton and derivatives of such compounds possess many useful features as potential lead agents, including high affinity and selectivity for the target receptors [44]. Compounds such as the two leads identified here may have multiple actions on the cardiovascular system.

In conclusion, we have demonstrated the utility of applying CoMFA to a novel G-protein coupled serotonin receptor, the $5HT_7$ receptor. Similarities between this CoMFA model and that for the D_1 dopamine receptor suggest that the CoMFA approach can be applied to other systems including D_2 dopamine receptors. It will be of interest to compare CoMFA models for $5HT_7$ vs. $5HT_{1A}$ to see if the same relationship holds as that observed between the D_1 and D_2 dopamine receptors.

Acknowledgements

The present work was supported by NIH grants AG11084, RR08579, ES07784, MH54865.

References

1. Lovenberg, T.W., Baron, B.M., de Lecea, L., Miller, J., Prosser, R., Rea, M.A., Foye, P.E., Racke, M., Slone, A.L., Siegel, B.W., Daneilson, P.E., Sutcliffe, J.G. and Erlander, M.G., Neuron, 11 (1993) 449.
2. Brusniak, M.-Y., Pearlman, R.S., Neve, K.A. and Wilcox, R.E., J. Med. Chem., 39 (1996) 850.
3. Wilcox, R.E., Tseng, T., Brusniak, M.Y., Ginsburg, B., Pearlman, R.S., Teeter, M., DuRand, C., Starr S. and Neve, K.A., J. Med. Chem., 41 (1998) 4385.
4. Wilcox, R.E., Huang, W.-H., Brusniak, M.-Y.K., Wilcox, D.M., Pearlman, R.S., Teeter, M.M., Durand, C.J., Wiens, B.L. and Neve, K.A., J. Med. Chem., 43 (2000) 3005.
5. Alexander, S. and Peters, J.A., TiPS Receptor & Ion Channel Nomenclature Supplement, 2000, Elsevier, Amsterdam.
6. Eglen, R.M., Jasper, J.R., Chang, D.J. and Martin, G.R., The 5-HT7 receptor: Orphan Found. Current Awareness, 1997.
7. Jasper, J.R., Kosaka, A., To, Z.P. and Chang, D.J.E., Brit. J. Pharmacol., 122 (1997) 126.
8. Ruat, M., Traiffot, E., Leurs, R., Tardivel-Lacombe, J., Diaz, J., Arrang, J. and Schwarz, J., Pharmacology, 90 (1993) 8547.
9. Shen, Y., Monsma, J., Metcalf, M.A.? Jose, P.A., Hamblin, M.W. and Sibley, D.R., J. Biol. Chem., 24 (1993) 18200.
10. Tsou, A., Kosaka, A., Bach, C., Zuppan, P., Yee, C., Tom, L., Alvarez, R., Ramsey, S., Bonhaus, D.W., Stefanich, E., Jakeman, L., Eglen, R.M. and Chan, H.W., J. Neurochem., 63 (1994) 456.
11. Bard, J.A., Zgombick, J., Adham, N., Vaysse, P., Branchek, T.A. and Weinshank, R.L., Am. Soc. Biochem. Molec. Biol., 268 (1993) 23422.

12. Hamel, E., Can. J. Neurol. Sci., 26 (1999) S2.
13. Meltzer, H.Y. Neuropsychopharmacology, 21 (1999) 106S.
14. Mullins, U.L., Gianutsos, G. and Eison, A.S., Neuropsychopharmacology, 21 (1999) 352.
15. Prins, N.H., Briejer, M.R., Van Bergen, P.J., Akkermans, L.M. and Schuurkes, J.A., Brit. J. Pharmacol., 128 (1999) 849.
16. Cushing, D.J., Zgombick, J.M., Nelson, D.L. and Cohen, M.L., J. Pharmacol. Exp. Ther., 277 (1996) 1560.
17. Salomon, Y., Adv. Cyclic Nucl. Res., 10 (1979) 35.
18. Fleming, W.W., Westfall, D.P., De La Lande, I.S. and Jehlett, L.B., J. Pharmacol. Exp. Ther., 181 (1972) 339.
19. Pearlman, R.S., Chem. Design Auto. News, 2 (1987) 1.
20. Pearlman, R.S., 3D QSAR in Drug Design. Theory Methods and Applications. ESCOM, Leiden, 1993.
21. TRIPOS, SYBYL User's Manuel. TRIPOS Inc, St. Louis, MO, 1998.
22. Wishart, G., Bremner, D.H. and Sturrock, K.R., Receptors Channels, 6 (1999) 317.
23. Neve, K.A. and Neve, R.L., The Dopamine Receptors. Humana Press, Clifton, New Jersey, 1997.
24. Marshall, G.R., Barry, D.C., Bosshard, H.E., Dammkoehler, R.A. and Dunn, D.A., in Olsen, E.C. (Ed.), Computer-Assisted Drug Design, Am. Chem. Soc., Washington, D.C., pp. 205–226.
25. Green, S.M. and Marshall, G.R., Trends Pharmacol. Sci, 16 (1995) 285.
26. Folkers, G., Merz, A. and Rognan, R., in Kubinyi, H. (Ed.), 3D-QSAR in Drug Design. Theory, Methods and Applications. Escom Leiden, pp. 583–618.
27. Dunn, W.J., Wold, S., Edlund, V. and Helberg, S., Quant. Struct. Act. Rel., 3 (1984) 131.
28. Cramer, R.D.d., Redl, G. and Berkoff, C.E., J. Med. Chem., 17 (1974) 533.
29. Cramer, R.D.d., Snader, K.M., Willis, C.R., Chakrin, L.W., Thomas, J. and Sutton, B.M., J. Med. Chem., 22 (1979) 714.
30. Marshall, G.R. and Cramer, R.D.d., Trends Pharmacol. Sci., 9 (1988) 285.
31. Cramer, R.D.d., Patterson, D.E. and Bunce, J.E., Progr. Clin. Biol. Res., 291 (1989) 161.
32. Cramer, R.D.I., Depriest, S., Patterson, D. and Hecht, P. in Kubingi, H. (Ed.), 3D QSAR in Drug Design. Theory, Methods, and Applications. ESCOM, Leiden, 1993, pp. 443–485.
33. Martin, Y.C., Methods Enzymol., 203 (1991) 587.
34. Wilcox, R.E., Gonzales, R.A. and Miller, J.D., in Nemeroff, C.B. (Ed.), Textbook of Psychopharmacology, American Psychiatric Press, New York, NY, pp. 3–36.
35. Hoyer, D., Clarke, D., Forzard, J.R., Hartig, P.R., Martin, G.R., Mylecharane, E.J., Saxena, P.R. and Humphrey, P.P.A., Pharmacol. Rev., 46 (1994) 157.
36. Agarwal, A. and Taylor, E.W., J. Comp. Chem., 14 (1993) 237.
37. Kuipers, W., van Wijngarden, I. and Ijzerman, A.P., Drug Design Discovery, 11 (1994) 231.
38. Chanda, P.K., Minchin, M.C.W., Davis, A.R., Greenberg, I., Reilly, Y., McGregor, W.H., Bhat, R., Lubeck, M.D., Mizutani, S. and Hung, P.P., Molec. Pharmacol., 43 (1993) 516.
39. Haak, L., Heller, H. and Pol v.d., A.N., J. Neurosci., 17 (1997) 1825.
40. Hamblin, M., Guthrie, C., Kohen, R. and Heidmann, D., Ann. N.Y. Acad. Sci., 861 (1998) 31.
41. Wilcox, R.E., in Craighead, W. and Nemeroff, C. (Eds), Encyclopedia of Psychology & Neuroscience. John Wiley, New York, NY, 1999.
42. Barnes, N.M. and Sharp, T., Neuropharmacology, 38 (1999) 1083.
43. Lovell, P.I., Bromidge, S.M., Dabbs, S., Duckworth, D.M., Forbes, I.T., Jennings, A.I., King, F.D., Middlemiss, D.N., Rahman, S.K., Saunders, D.V., Collin, L.L., Hagan, J.J., Riley, G.J. and Thomas, D.R., J. Med. Chem., 43 (2000) 342.
44. Mantegani, S., Brambilla, E. and Varasi, M., Il Farmaco, 54 (1999) 288.
45. Cheng, Y. and Prusoff, W.H., Biochm. Pharmacol., 22 (1973) 3099.